

NACA RM No. L8B20 340

FILE COPY
NO 2

★ CONFIDENTIAL

Copy No. 176

RM No. L8B20



RESEARCH MEMORANDUM

FREE-FLIGHT-TUNNEL TESTS OF A TARGET-SEEKING GLIDE-BOMB
MODEL WITH FLICKER LATERAL CONTROL

By

Marion O. McKinney, Jr., and Hubert M. Drake

Langley Aeronautical Laboratory
Langley Field, Va.

THIS DOCUMENT ON LOAN FROM THE FILES OF

NATIONAL ADVISORY COMMITTEE FOR AERONAUTICS
LANGLEY AERONAUTICAL LABORATORY
LANGLEY FIELD, HAMPTON, VIRGINIA

CLASSIFIED DOCUMENT

RETURN TO THE ABOVE ADDRESS.

This document contains classified information affecting the National Defense of the United States within the meaning of the Espionage Act, USC 50:31 and 32. Its transmission or the revelation of its contents in any manner to an unauthorized person is prohibited by law. Information so classified may be imparted only to persons in the military and naval services of the United States, appropriate civilian officers and employees of the Federal Government who have a legitimate interest therein, and to United States citizens of known loyalty and discretion who of necessity must be informed thereof.

REQUESTS FOR PUBLICATIONS SHOULD BE ADDRESSED AS FOLLOWS:

NATIONAL ADVISORY COMMITTEE FOR AERONAUTICS
1512 H STREET, N. W.
WASHINGTON 25, D. C.

NATIONAL ADVISORY COMMITTEE FOR AERONAUTICS

WASHINGTON

July 28, 1948

CONFIDENTIAL



NATIONAL ADVISORY COMMITTEE FOR AERONAUTICS

RESEARCH MEMORANDUM

FREE-FLIGHT-TUNNEL TESTS OF A TARGET-SEEKING GLIDE-BOMB

MODEL WITH FLICKER LATERAL CONTROL

By Marion O. McKinney, Jr., and Hubert M. Drake

SUMMARY

The NACA has been investigating control systems suitable for target-seeking missiles. As part of this program, tests have been made in the Langley free-flight tunnel on a model of the GB-5 glide bomb equipped with a light-seeker control unit which applied control in response to deviations in sidewise displacement and angles of bank and yaw. The seeker applied flicker control; that is, the control was full on to the right or left when the deviation exceeded the deadspot and full off when the deviation was within the deadspot.

The results of this investigation showed that good stability could be obtained with the flicker-type control system. The model was somewhat less stable with the flicker control system, however, than with a proportional control system previously tested in the Langley free-flight tunnel. Increasing the sensitivity of the control system to bank or increasing the ratio of rudder travel to aileron travel improved the stability of the model.

INTRODUCTION

Recently the NACA has been participating in a research program to obtain satisfactory control systems for pilotless aircraft. It was believed that considerable simplification of guided-missile control systems would be possible if satisfactory flight characteristics could be obtained with a flicker, or on-off, type of control. An investigation has been conducted, therefore, in the Langley free-flight tunnel to determine the flying characteristics of a model having an automatic flicker lateral control system and to compare the flying characteristics obtained with the flicker control system with those previously obtained with a proportional control system in the same model (reference 1).

The $\frac{1}{4}$ -scale model of the Aeronca GB-5 previously used in the proportional control study was used in the present investigation. The model was equipped with a light-sensitive target seeker which caused

the ailerons and rudders to deflect in response to angular deviations in bank and yaw and to sidewise displacement from the target line. Flight tests were made with 2° deadspot for a range of values of the ratio of rudder travel to aileron travel and for various degrees of sensitivity to bank. Several additional flight tests were made with the deadspot increased to 10° .

SYMBOLS

All forces and moments are referred to the stability axes which are illustrated and defined in figure 1.

m	mass
S	wing area, square feet
q	dynamic pressure, pounds per square foot $\left(\frac{1}{2}\rho V^2\right)$
b	wing span, feet
k_X	radius of gyration about longitudinal body axis through center of gravity, feet
k_Z	radius of gyration about normal body axis through center of gravity, feet
V	airspeed, feet per second
ρ	mass density of air, slugs per cubic foot
r	yawing angular velocity, radians per second
ψ	angle of yaw, degrees
ϕ	angle of bank, degrees
y	sidewise displacement, feet
δ_a	aileron deflection, degrees
δ_r	rudder deflection, degrees
δ_s	angle between X-Z plane of target seeker and straight line from seeker to target
x	aileron control gearing, ratio of aileron deflection to seeker deflection angle δ_a/δ_s for proportional control system described in reference 1

- z rudder control gearing, ratio of rudder deflection to seeker deflection angle δ_r/δ_s for proportional control system described in reference 1
- d distance from target, feet
- τ angle of target light above flight path of model, degrees
- μ relative-density factor ($m/\rho S b$)
- C_Y lateral-force coefficient (Lateral force/ qS)
- C_L lift coefficient (Lift/ qS)
- C_n yawing-moment coefficient (Yawing moment/ qSb)
- C_l rolling-moment coefficient (Rolling moment/ qSb)
- $C_{n\beta}$ rate of change of yawing-moment coefficient with angle of sideslip in degrees ($\partial C_n/\partial \beta$)
- $C_{l\beta}$ rate of change of rolling-moment coefficient with angle of sideslip in degrees ($\partial C_l/\partial \beta$)
- $C_{Y\beta}$ rate of change of lateral-force coefficient with angle of sideslip in degrees ($\partial C_Y/\partial \beta$)
- C_{n_r} rate of change of yawing-moment coefficient with yawing-angular-velocity factor $\left(\frac{\partial C_n}{\partial \frac{rb}{2V}}\right)$
- $C_{l\delta_a}$ rate of change of rolling-moment coefficient with aileron deflection in degrees ($\partial C_l/\partial \delta_a$)
- $C_{n\delta_a}$ rate of change of yawing-moment coefficient with aileron deflection in degrees ($\partial C_n/\partial \delta_a$)
- $C_{n\delta_r}$ rate of change of yawing-moment coefficient with rudder deflection in degrees ($\partial C_n/\partial \delta_r$)

Subscripts l and r refer to the right and left rudder, respectively.

APPARATUS

Tunnel and Model

The investigation described herein was conducted in the Langley free-flight tunnel, which is designed to test unrestrained models in flight. A complete description of the tunnel and its operation is presented in reference 2. A photograph of the glide-bomb model flying in the test section of the tunnel is presented as figure 2.

The $\frac{1}{4}$ -scale model used in the tests was geometrically similar to the Aeronca GB-5 controllable glide bomb except that the airfoil section of the model wing was the Rhode St. Genese 35 which is an airfoil that gives a good value of maximum lift at low scale. The mass characteristics of the model, however, were not scaled down from the GB-5 inasmuch as the low airspeed of the tunnel limited the wing loading of the model to a low value. The weight of the model was 6.3 pounds and the moments of inertia I_X and I_Z were 0.087 and 0.136 slug-foot², respectively. A sketch of the model giving the pertinent dimensions is presented as figure 3. This is the same model which was used in previous investigation with a target seeker which provided proportional control.

Target Seeker

The lateral-control unit of the full-scale GB-5 consisted of a target seeker to guide the bomb toward the target by applying control in response to deviations in yaw and sidewise displacement and consisted of a tilted gyroscope to provide automatic stabilization in bank and yaw. The size and weight of the full-scale control unit prohibited its use in the free-flight-tunnel model, and construction of a scale model of the control unit was considered impractical. Hence, a control unit consisting solely of a target seeker was developed for this project at the Langley Laboratory. The primary function of the gyroscope (providing automatic stabilization in bank) was performed by the seeker, however, by the expedient of mounting the target above the flight path of the model. With this arrangement, the seeker applied control in response to bank as well as yaw and sidewise displacement. The angle at which the target was located above the flight path is referred to herein as the angle of tilt, inasmuch as the effect of this angle on the motion of the controls roughly corresponds to the angle of tilt of a tilted gyroscope. The seeker, however, did not give exactly the same type of control as the target-seeker and gyroscope unit of the full-scale glide bomb would give.

The target seeker used for the free-flight-tunnel tests was essentially a light-sensitive device which applied full control when the model deviated from the target line. A schematic diagram of the seeker and control system is presented in figure 4. This system consisted of

two photoelectric tubes mounted behind a shield with a fixed slit, an amplifier, and relays which controlled the current to the electromagnetic control-actuating mechanisms.

The operation of the seeker was as follows: The light from the light source (simulating the target) entered the shield through the slit and fell upon the photoelectric tubes; the electrical output of the two photoelectric tubes (which is proportional to the light intensity on the tubes) was amplified and any difference between the output of the two tubes was used to actuate relays which applied current to the proper side of the electromagnetic servo and thus moved the airplane controls in such a way as to turn the model toward the target.

This target seeker had a deadspot (range of angles through which the device could not detect a deviation), and the controls remained at neutral when the deviations from the target line were within the deadspot as illustrated in figure 5(a).

The target seeker also had some inherent lag because the relays and servos were not instantaneous in their operation. The lag in the system was measured on a rocking table and was determined to be 0.05 second. The effect of lag on the response of the controls to a sinusoidal motion of the model is shown in figure 5. Lag caused the deadspot to shift in the direction of the motion of the model and caused the size of the deadspot to increase. Both of these effects became more pronounced as the angular velocity of the model increased.

The angle to which the target seeker was sensitive was the angle δ_s between the X-Z plane of the seeker and the plane which included the flight-path axis and the target light. This angle is illustrated in figure 6. The variation of the angle δ_s with the angle of yaw and side-wise displacement were equal to $-\psi$ and $-\tan^{-1} \frac{y}{d}$, respectively. The variation of δ_s with the angle of bank was equal to $-\tan^{-1} \sin \phi \tan \tau$, which may be closely approximated by the expression $\phi \sin \tau$ for angles of tilt from 0° to 40° . Combining the effects of the angles of bank and of yaw and the sidewise displacement on the angle, then, δ_s may be expressed as

$$\delta_s = -\phi \sin \tau - \psi - \tan^{-1} \frac{y}{d}$$

The first term $-\phi \sin \tau$ represents the bank stabilization which would normally be provided by a gyro system and the second and third terms $-\psi - \tan^{-1} \frac{y}{d}$ represent the guidance which would normally be supplied by a target seeker.

The portion of the angle δ_s which results from sidewise displacement $-\tan^{-1} \frac{y}{d}$ is inversely proportional to the distance from the bomb to the target. In the Langley free-flight tunnel, this distance was a constant value of about 15 feet (60 ft, full scale). Inasmuch as the full-scale bomb during most of its flight would be at a much greater distance from the target, it would get less response to sidewise displacement than in the free-flight-tunnel tests.

The model had a longitudinal target seeker which provided automatic longitudinal control. This seeker was the same one that was used for lateral control in the investigation of reference 1. To use this seeker as a proportional longitudinal control device it was mounted on its side and connected to the elevator. This target seeker is fully described in reference 1. Essentially, it consisted of a pair of photoelectric tubes mounted behind a light shield with a slit. The light shield could rotate in pitch and was driven by a servo motor in such a manner as to keep the shield pointed at the target light. The motion of the shield was transmitted to the elevator by means of control cables. The control was set before take-off so that when the model was flying in the proper position in the tunnel, the desired values of airspeed and angle of tilt would be obtained.

This longitudinal seeker was used during the present tests purely as a convenience in that it provided longitudinally steady flights. No investigation was made of the longitudinal characteristics of the model. With this seeker the model flew satisfactorily with an elevator gearing ratio (ratio of elevator deflection to seeker deflection) of 2.0 and no changes in linkage were made. At a constant airspeed the vertical variations from the average flight path were less than 3 inches.

Recording Apparatus

Records of the lateral motions of the model were made by means of motion-picture cameras which were located at the top and rear of the tunnel and were aimed along the longitudinal and normal axis of the tunnel. Records of the control movements were made on the camera records by the flashing of a pair of argon lights which were located in the common field of the two cameras. These lights were connected to the lateral-control mechanism so that one of the lights was turned on while current was being supplied to the right control servos and the other light was turned on when current was being supplied to the left control servos. The cameras were run at 16 frames per second and the motions of the model and controls were determined by reading the movie records frame by frame. By this means it was possible to fair reasonably accurate records of the motions of the model. The motions of the controls could not be determined accurately, however, because the movie records showed only whether the control servos were energized at intervals of $\frac{1}{16}$ second. The deflection of the controls caused by the servo mechanisms was determined from preflight measurements of the deflections at zero airspeed.

This method of recording the motions of the model and controls was not completely satisfactory. The motion-picture records were of rather poor quality and difficult to read because there was insufficient light in the tunnel during the tests to expose the film properly. The only light used in the tunnel was the target because the light from the normal illuminating system was found to cause the light-sensitive target seeker to function improperly. The records of the control movements were not entirely satisfactory, because of the rather large time intervals between measurements and because the control angle was not recorded directly.

The angular deadspot of the target seeker was determined experimentally by measuring the distance that a light source a known distance ahead of the model could be moved sidewise without energizing the model controls.

TESTS

In the flight tests, the model was flown at a predetermined tilt angle and airspeed by the automatic longitudinal-control mechanism while the flicker lateral-control mechanism controlled the lateral motions of the model. If the automatic control proved to be destabilizing, the free-flight-tunnel pilot was able to override it and prevent a crash. Motion-picture records of the lateral motions of the model were made for each of the various test conditions.

The values of the different parameters varied in the course of the tests are given in table I. For all of the tests the total aileron deflection used for control was 30° (± 15). The model was flown with 2° deadspot for a range of values of tilt angle and rudder deflection as shown in figure 7. Several flights were also made with 10° deadspot. The ratio of rudder deflection to aileron deflection was varied by changing the rudder control linkage to vary the rudder deflection caused by a control signal. Only the left rudder was used for the majority of the tests although both rudders were used for three of the test conditions where more yawing moment was desired than could be supplied by one rudder. All of the flight tests were made at a lift coefficient of 0.64.

The low airspeed available in the Langley free-flight tunnel made it impossible to test a model having a wing loading as high as the scaled-down wing loading of the full-scale glide bomb. The results of the tests are considered directly applicable only for a full-scale airplane or missile having the scaled-up mass characteristics of the model.

Force tests were made to determine the static stability and control characteristics of the model. The value of the damping-in-yaw derivative C_{n_r} for the model is given in reference 1 as -0.226. The damping-in-roll derivative C_{l_p} of the wing alone has been measured and is given in reference 3 as -0.30.

RESULTS AND DISCUSSION

The results of the force tests to determine the static stability and control characteristics of the model are presented in figure 8.

The results of the flight tests are presented in the form of time histories of the motions of the model in figures 9 to 26. During the time that these records were made, the model was controlled only by the target seeker; the free-flight-tunnel pilot did not handle the controls. In some of these time histories there is no record of the yawing motions of the model because the film was not readable. The records of the control motions are also missing on some of the time histories because of improper functioning of the control-indicator lights.

The motions of the model for the most stable conditions were characterized by a wandering motion rather than by a steady hunting oscillation. Apparently the model moved around in the deadspot for a considerable part of the time. When it wandered out of the deadspot, the control deflection moved the model back but with so little force that it often was not moved back all the way through the deadspot. As the model became less stable a more definite oscillation was evident. In general, however, the motions of the model with the flicker-control mechanism were not as smooth and steady as the oscillations obtained with the proportional control system discussed in reference 1. This fact may be ascertained from figure 27 which shows the motions of the model for two of the best conditions covered in the proportional study (reference 1) compared with two of the best conditions covered in the present investigation.

An improvement in the stability and a decrease in the amplitude of the hunting oscillations of the model were obtained by increasing the angle of tilt and thereby increasing the sensitivity of the target seeker to the angle of bank. This result is illustrated in figures 28, 29, and 30 in which time histories of the rolling motions of the model have been reproduced to show the effects of varying the angle of tilt for approximately constant values of rudder deflection. These figures show that the angle of tilt required to give stability increased as the rudder travel was reduced.

The angle of tilt was a very important factor affecting the stability because it provided for an immediate response to deviations in bank. If there were no response to the angle of bank, correction of a deviation in bank would be delayed until the yawing and sideslipping, which followed the rolling, developed sufficiently to cause the proper control movement to correct the bank. Such a delay in correcting rolling would cause the stability to be considerably worse than if there was an immediate correction for the rolling.

Increasing the rudder travel so as to increase the ratio of rudder movement to aileron movement caused an improvement in the stability and a decrease in the amplitude of the hunting oscillations. This result is

illustrated in figures 31, 32, and 33 which show the effects of varying the rudder travel at constant angles of tilt. These figures show that the amount of rudder travel used had little effect on the stability of the model for the largest angle of tilt ($\tau = 42^\circ$) but became more important as the tilt angle was decreased.

The effects of the angle of tilt and the rudder travel have been summarized briefly in figure 34 which shows the experimentally determined stability boundary. In some of the cases which have been termed unstable on this figure the motion might have been a constant-amplitude hunting oscillation, the amplitude of which was greater than the size of the tunnel. It is believed, however, that the stability boundary is fairly representative of the effect on the stability of varying the angle of tilt and rudder travel.

The characteristics of the proportional control system previously tested in the Langley free-flight tunnel are illustrated in figure 35 which presents some of the time histories of rolling motions taken from reference 1. Comparison of the results of the present flicker-control investigation with those of the proportional-control investigation shows that in both cases increasing the angle of tilt improved the stability of the model. With the proportional system, however, it was found that there was an optimum rudder travel of about one-half the aileron travel, whereas in the present investigation increasing the rudder travel was found to be beneficial in all cases covered ($\frac{\delta_r}{\delta_a} \leq 2.30$).

A few flights were attempted with 10° deadspot. For all of the conditions covered in these tests, however, the motions of the model were so unstable that no flight records could be made.

CONCLUSIONS

The following conclusions were drawn from an investigation in the Langley free-flight tunnel of the lateral stability of a glide-bomb model having a flicker-type automatic control device.

1. Fairly good stability was obtained with the flicker-control system and the flying characteristics of the model were satisfactory.
2. The stability of the model with the flicker-control device was not as good as that previously obtained with the same model using an automatic proportional control system.
3. Increasing the sensitivity of the control system to bank by increasing the angle of tilt improved the stability of the model.
4. Increasing the ratio of rudder travel while keeping the aileron travel constant improved the stability of the model.

5. Increasing the deadspot from 2° to 10° caused the model to become so unstable that it could not be flown.

Langley Aeronautical Laboratory
National Advisory Committee for Aeronautics
Langley Field, Va.

REFERENCES

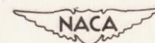
1. Drake, Hubert M., and McKinney, Marion O., Jr.: Free-Flight-Tunnel Tests of a Target-Seeking Glide-Bomb Model with Proportional Lateral Control. NACA MR No. L6C06, Army Air Forces, 1946.
2. Shortal, Joseph A., and Osterhout, Clayton J.: Preliminary Stability and Control Tests in the NACA Free-Flight Wind Tunnel and Correlation with Full-Scale Flight Tests. NACA TN No. 810, 1941.
3. Tosti, Louis P.: Low-Speed Static Stability and Damping-in-Roll Characteristics of Some Swept and Unswept Low-Aspect-Ratio Wings. NACA TN No. 1468, 1947.

TABLE I

TABLE OF TEST CONDITIONS

Test	Deadspot (deg)	Angle of tilt (deg)	Rudder deflection			Rudder yawing- moment coefficient (a)
			δ_{r_r} (deg)	δ_{r_l} (deg) (a)	Total (deg) (a)	
1	2	42	0	-10	-10	-0.0235
2	2	42	0	-5	-5	-.0164
3	2	42	0	0	0	0
4	2	42	0	10	10	.0235
5	2	42	0	20	20	.0403
6	2	42	0	35	35	.0598
7	2	32	0	0	0	0
8	2	32	0	10	10	.0235
9	2	32	0	20	20	.0403
10	2	32	0	35	35	.0598
11	2	26	0	10	10	.0235
12	2	20	0	0	0	0
13	2	20	0	10	10	.0235
14	2	20	0	25	25	.0464
15	2	20	0	35	35	.0598
16	2	8	20	20	40	.0806
17	2	8	35	35	70	.1196
18	2	0	20	20	40	.0806
19	10	42	0	20	20	.0403
20	10	42	0	35	35	.0598
21	10	32	0	20	20	.0403
22	10	32	0	35	35	.0598

^aMinus signs indicate that rudder deflections or yawing moments were in the direction opposite to the aileron deflections or yawing moments.



CONFIDENTIAL

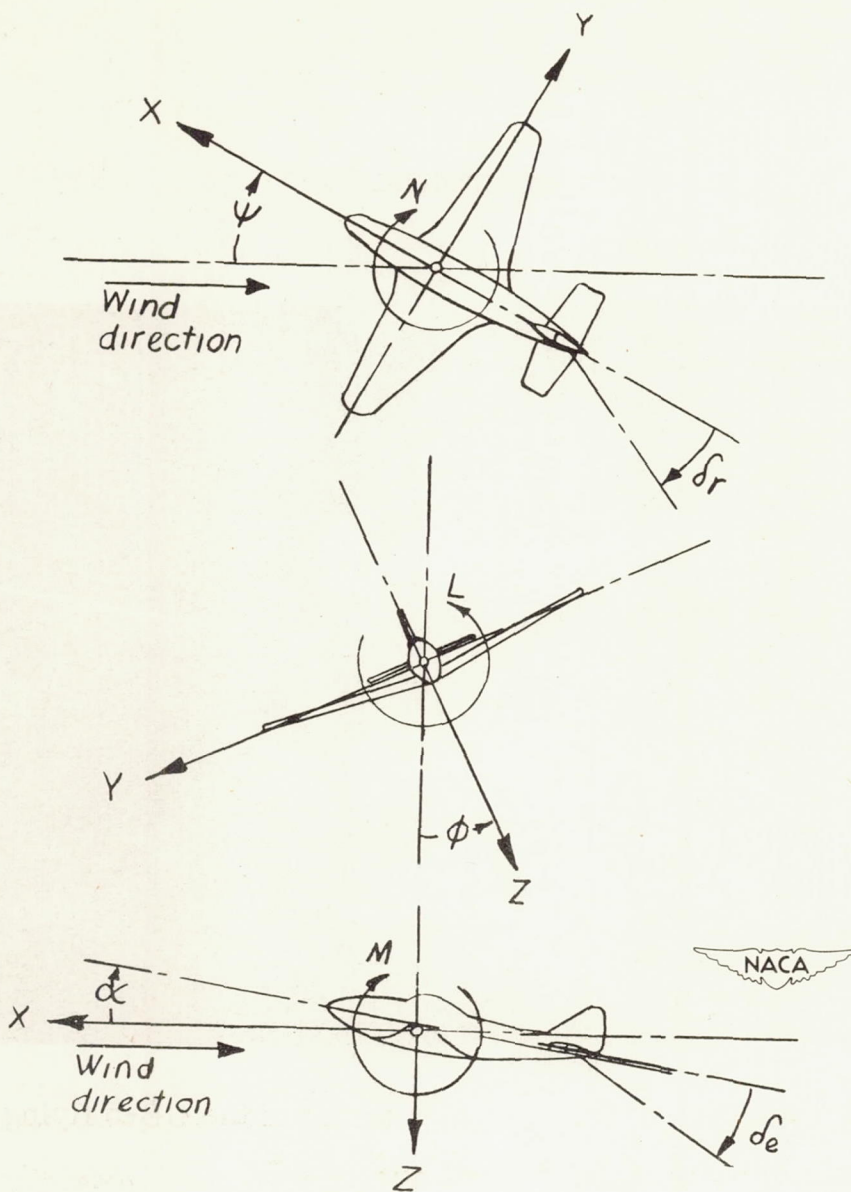


Figure 1.- The stability system of axes. Arrows indicate positive directions of moments, forces, and control-surface deflections. This system of axes is defined as an orthogonal system having the origin at the center of gravity and in which the Z-axis is in the plane of symmetry and perpendicular to the relative wind, the X-axis is in the plane of symmetry and perpendicular to the Z-axis, and the Y-axis is perpendicular to the plane of symmetry.

CONFIDENTIAL

CONFIDENTIAL

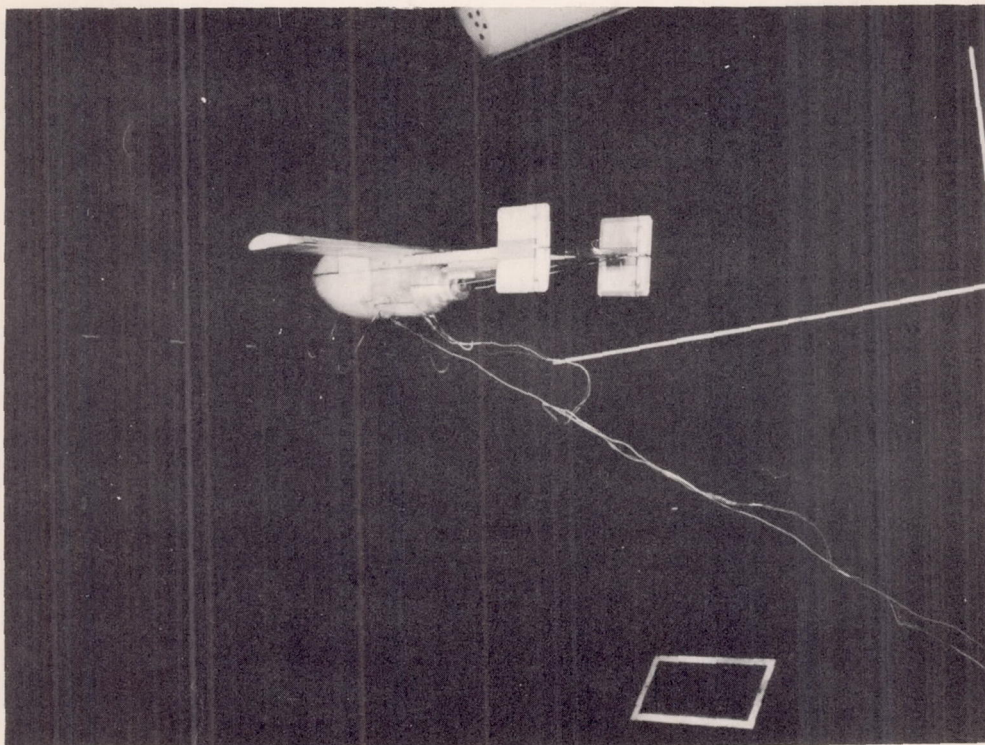
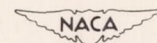


Figure 2.- Photograph of the $\frac{1}{4}$ -scale model of the GB-5 flying in the test section of the Langley free-flight tunnel.



L-39514

CONFIDENTIAL

Fig. 1

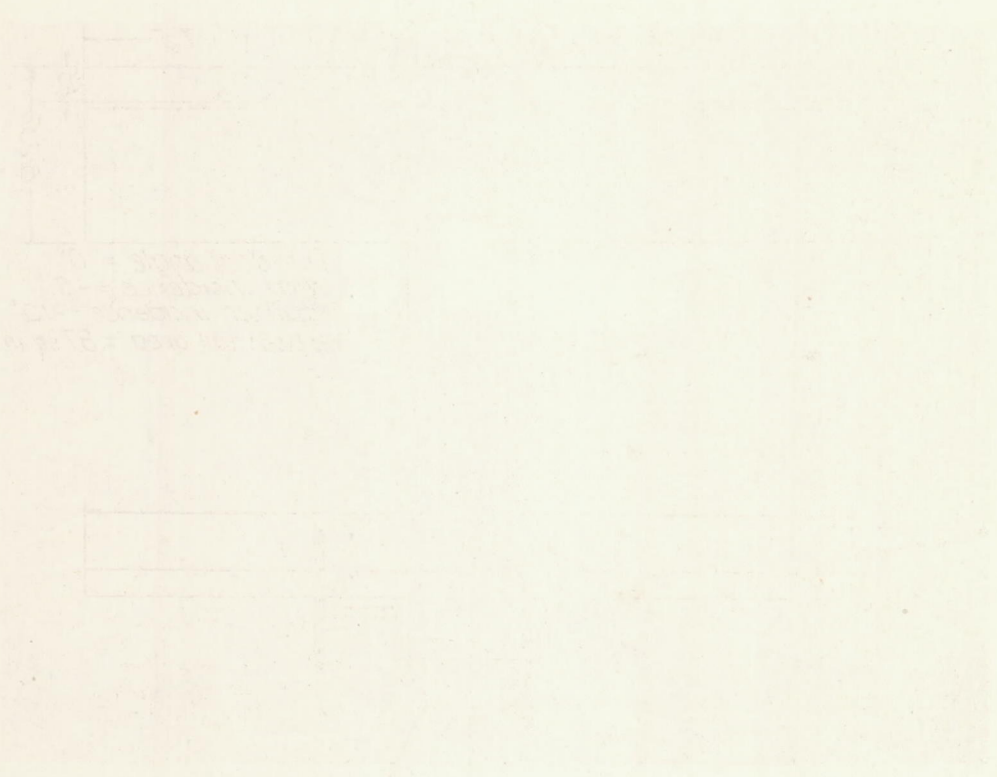
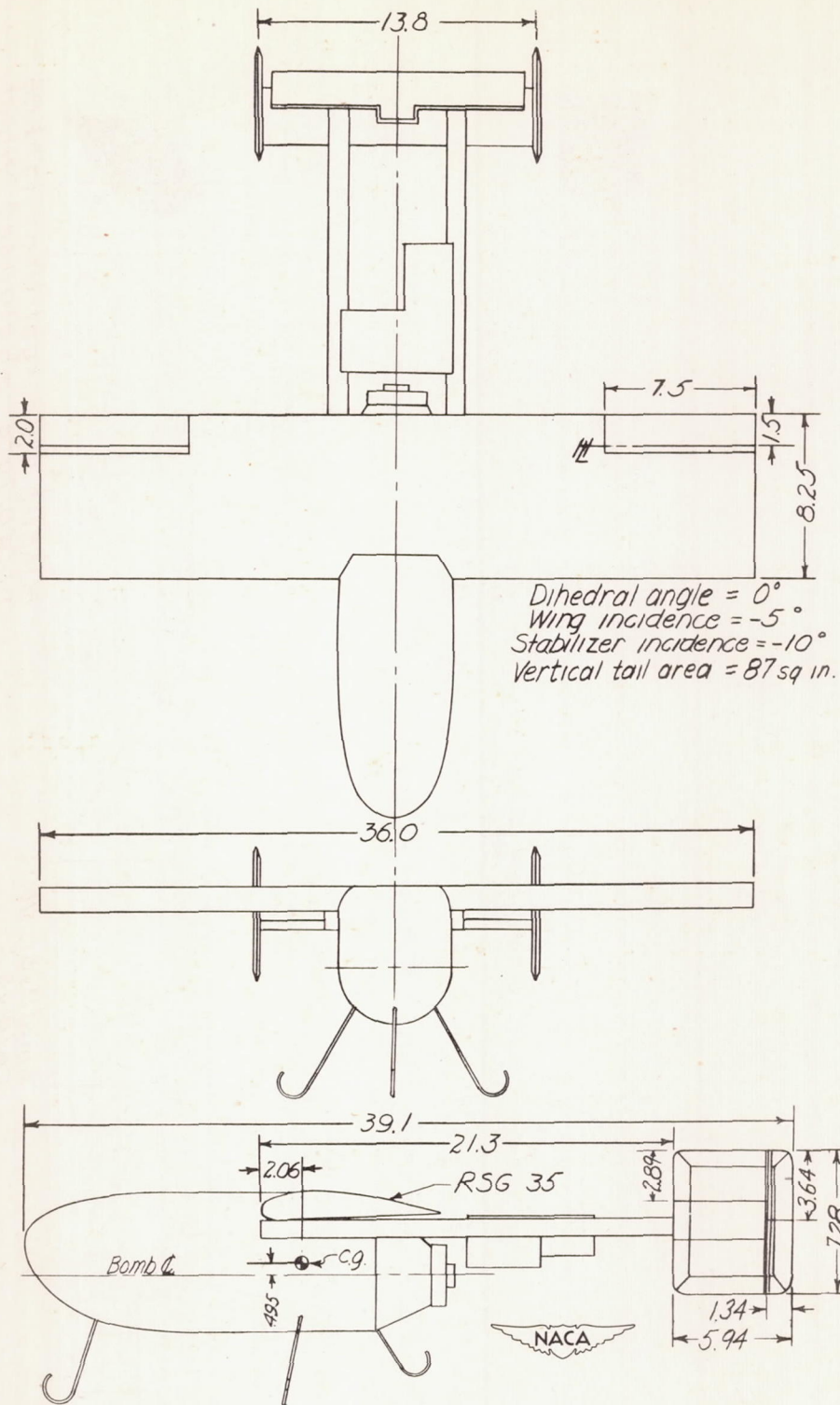


Fig. 2
 Fig. 3
 Fig. 4
 Fig. 5
 Fig. 6
 Fig. 7
 Fig. 8
 Fig. 9
 Fig. 10
 Fig. 11
 Fig. 12
 Fig. 13
 Fig. 14
 Fig. 15
 Fig. 16
 Fig. 17
 Fig. 18
 Fig. 19
 Fig. 20
 Fig. 21
 Fig. 22
 Fig. 23
 Fig. 24
 Fig. 25
 Fig. 26
 Fig. 27
 Fig. 28
 Fig. 29
 Fig. 30
 Fig. 31
 Fig. 32
 Fig. 33
 Fig. 34
 Fig. 35
 Fig. 36
 Fig. 37
 Fig. 38
 Fig. 39
 Fig. 40
 Fig. 41
 Fig. 42
 Fig. 43
 Fig. 44
 Fig. 45
 Fig. 46
 Fig. 47
 Fig. 48
 Fig. 49
 Fig. 50
 Fig. 51
 Fig. 52
 Fig. 53
 Fig. 54
 Fig. 55
 Fig. 56
 Fig. 57
 Fig. 58
 Fig. 59
 Fig. 60
 Fig. 61
 Fig. 62
 Fig. 63
 Fig. 64
 Fig. 65
 Fig. 66
 Fig. 67
 Fig. 68
 Fig. 69
 Fig. 70
 Fig. 71
 Fig. 72
 Fig. 73
 Fig. 74
 Fig. 75
 Fig. 76
 Fig. 77
 Fig. 78
 Fig. 79
 Fig. 80
 Fig. 81
 Fig. 82
 Fig. 83
 Fig. 84
 Fig. 85
 Fig. 86
 Fig. 87
 Fig. 88
 Fig. 89
 Fig. 90
 Fig. 91
 Fig. 92
 Fig. 93
 Fig. 94
 Fig. 95
 Fig. 96
 Fig. 97
 Fig. 98
 Fig. 99
 Fig. 100

CONFIDENTIAL



CONFIDENTIAL

Figure 3.- Three-view sketch of $\frac{1}{4}$ -scale model of the type GB-5 controllable glide bomb as tested in the Langley free-flight tunnel. All dimensions in inches.

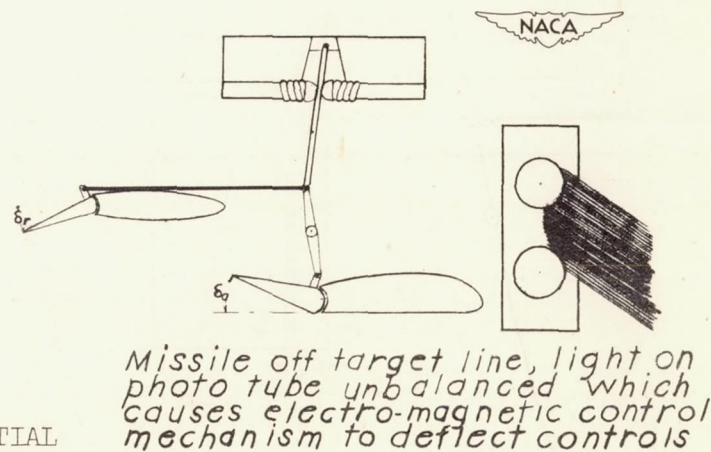
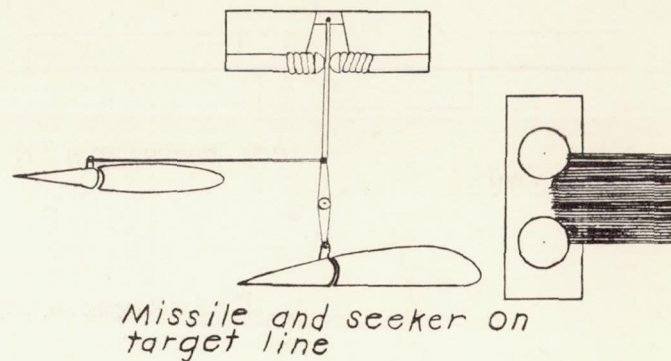
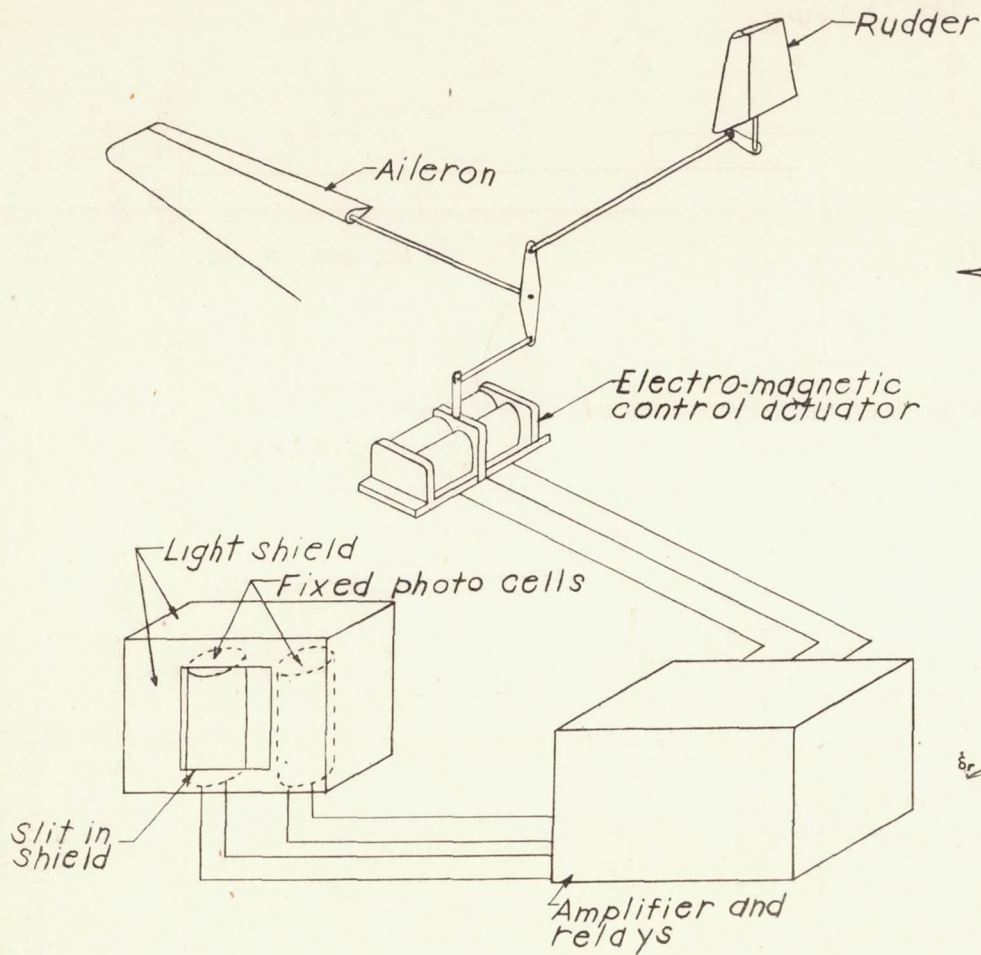


Figure 4.- The target seeker and its operation.

CONFIDENTIAL

NACA RM No. 18B20

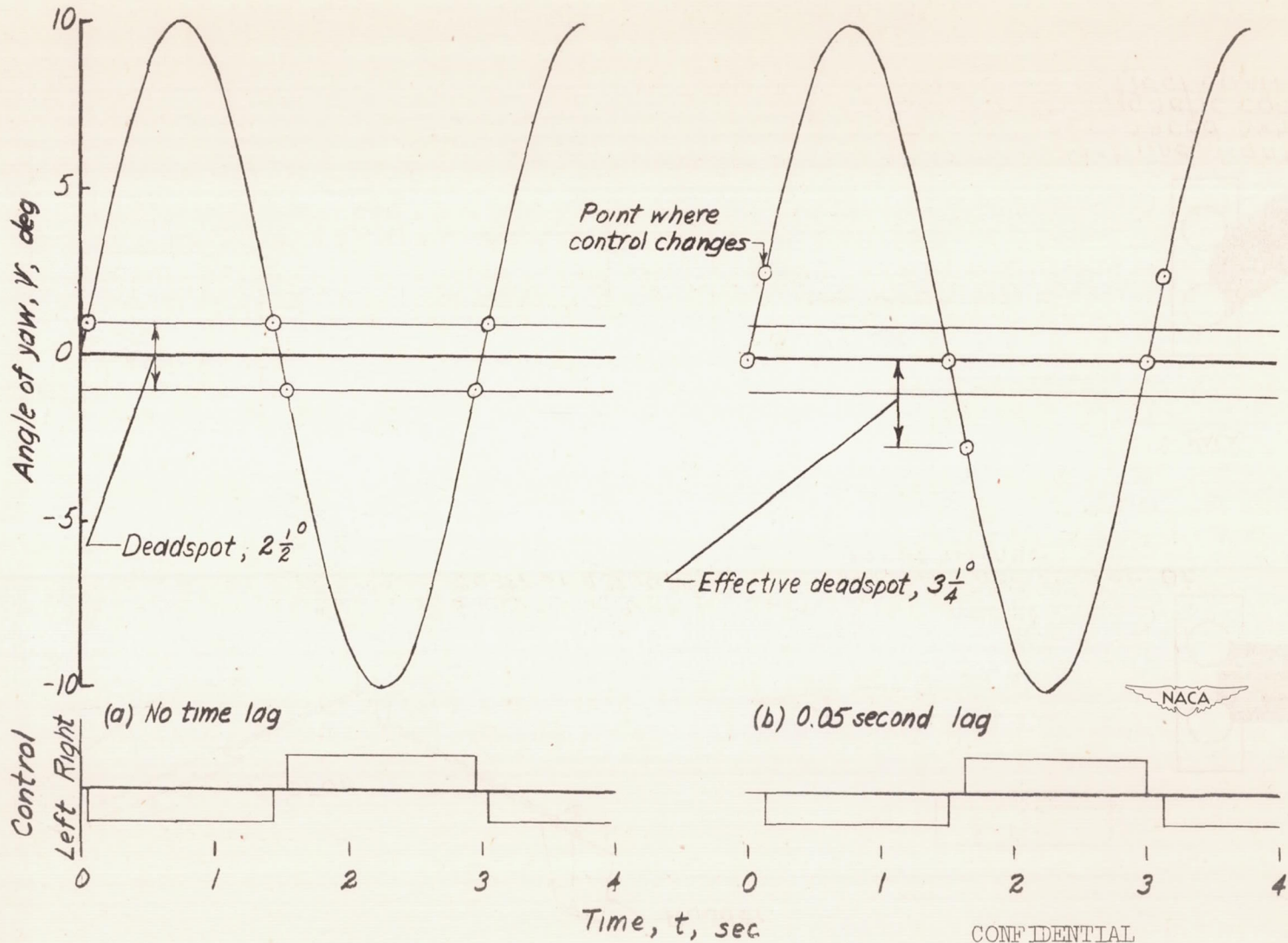
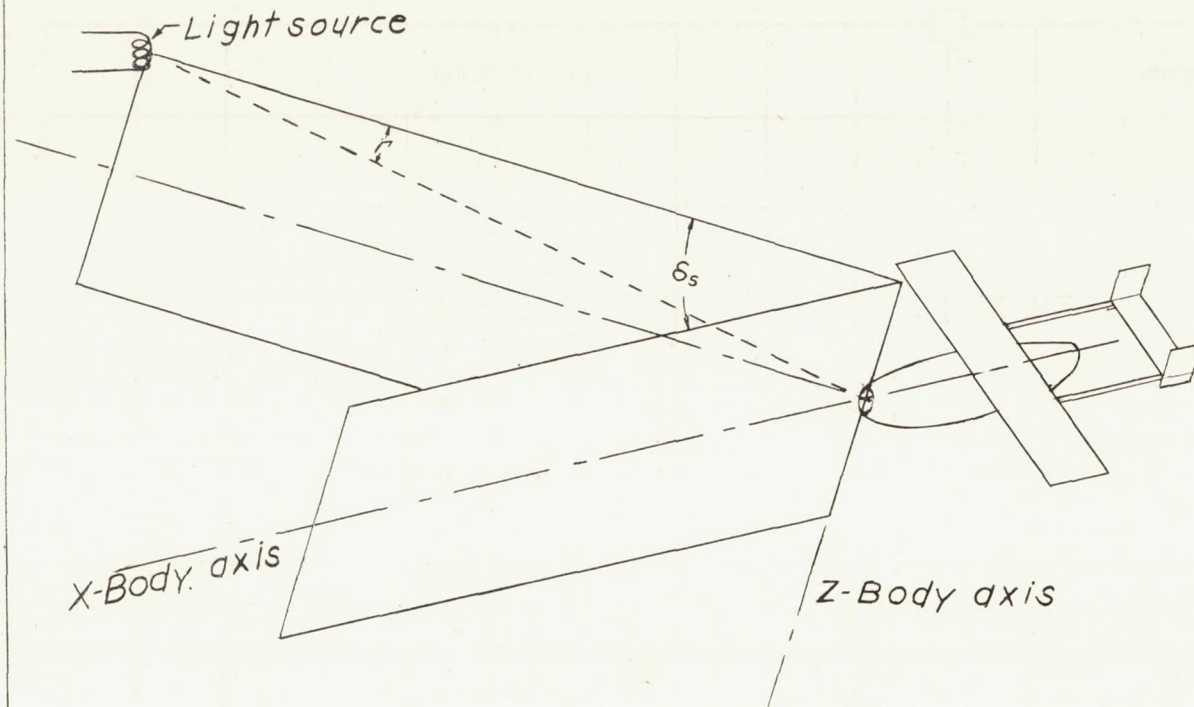


Figure 5.- Effect of time lag on model control application and effective dead spot.

CONFIDENTIAL



CONFIDENTIAL

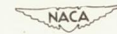


Figure 6.- Illustration of the angle δ_s to which the seeker is sensitive.

CONFIDENTIAL

NACA RM No. 18B20

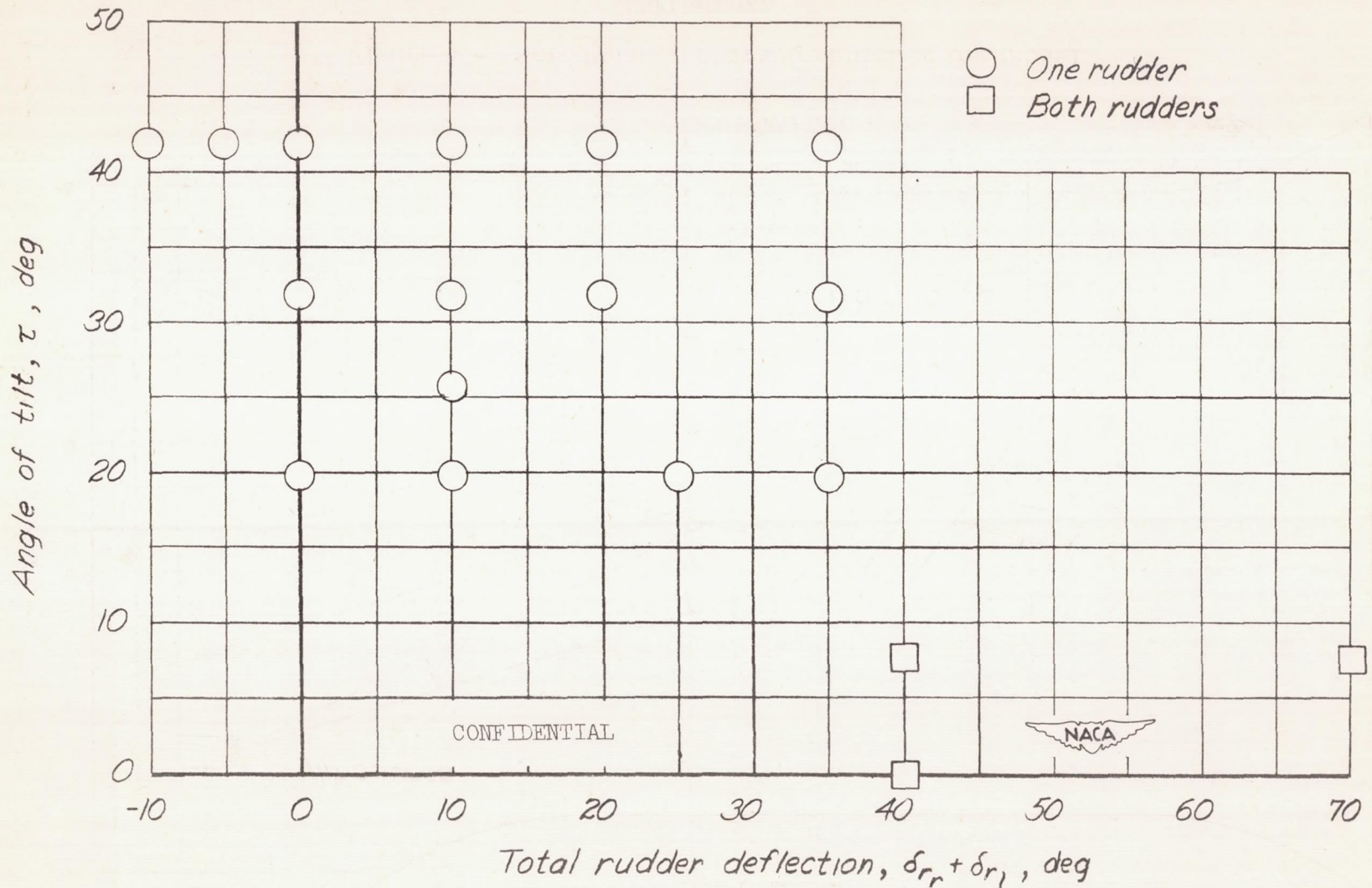


Figure 7.- Values of the angle of tilt and rudder deflection covered in the tests.

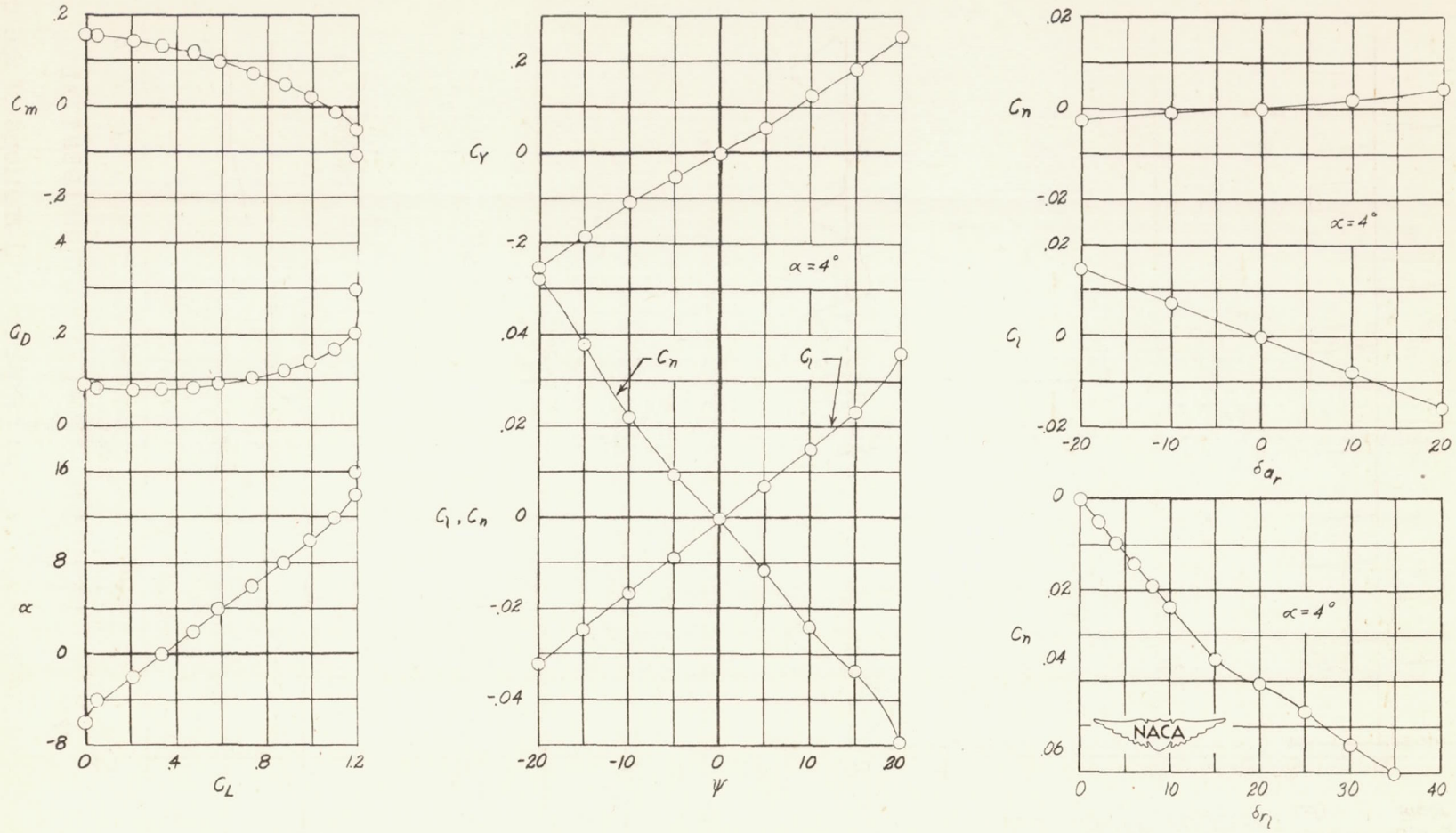


Figure 8.- Aerodynamic characteristics of the model.

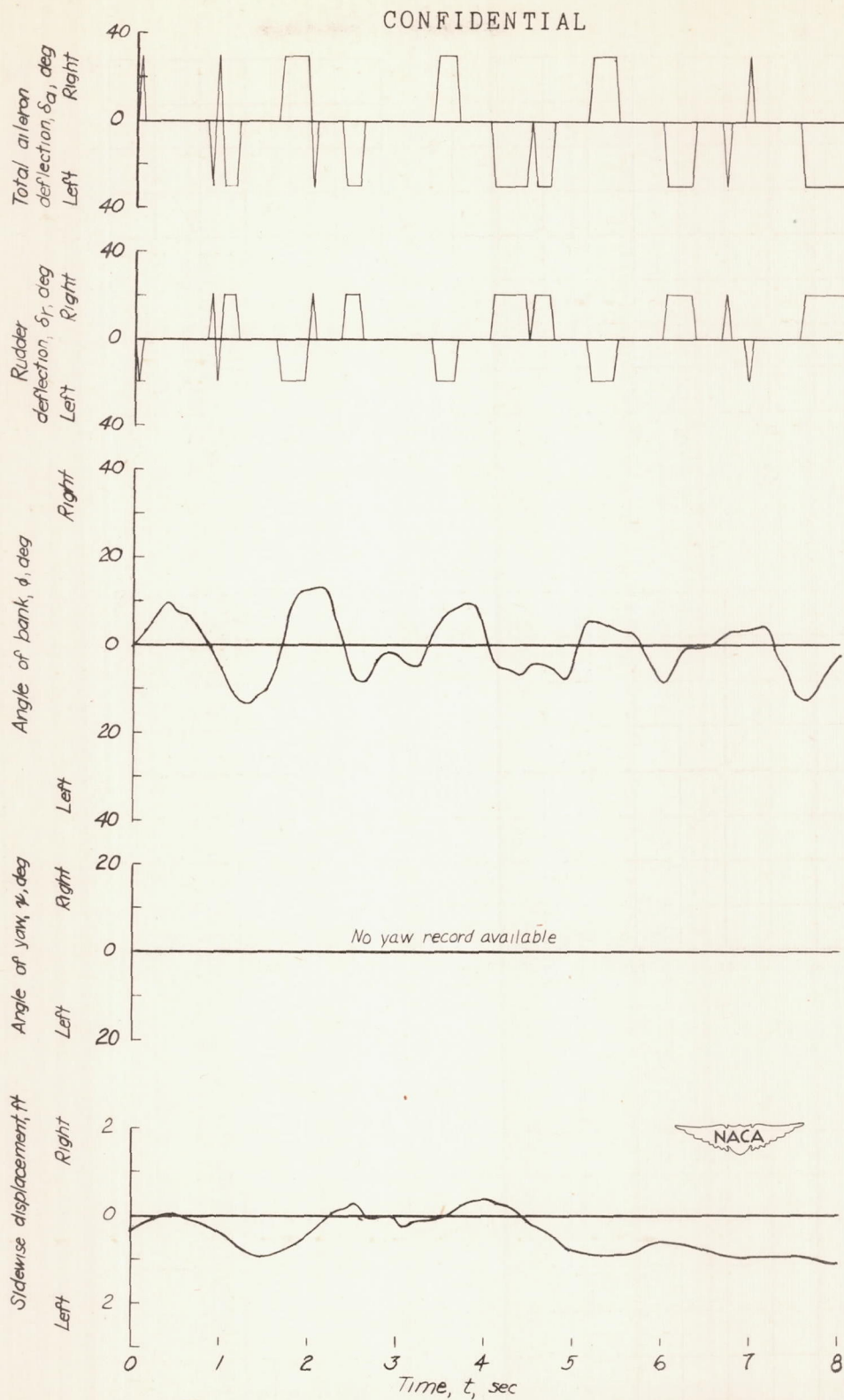


Figure 9.- Typical flight record of the lateral motions of the model for test 1 (right rudder fixed, left rudder moved 10° opposite to aileron movement, $\tau = 42^\circ$).

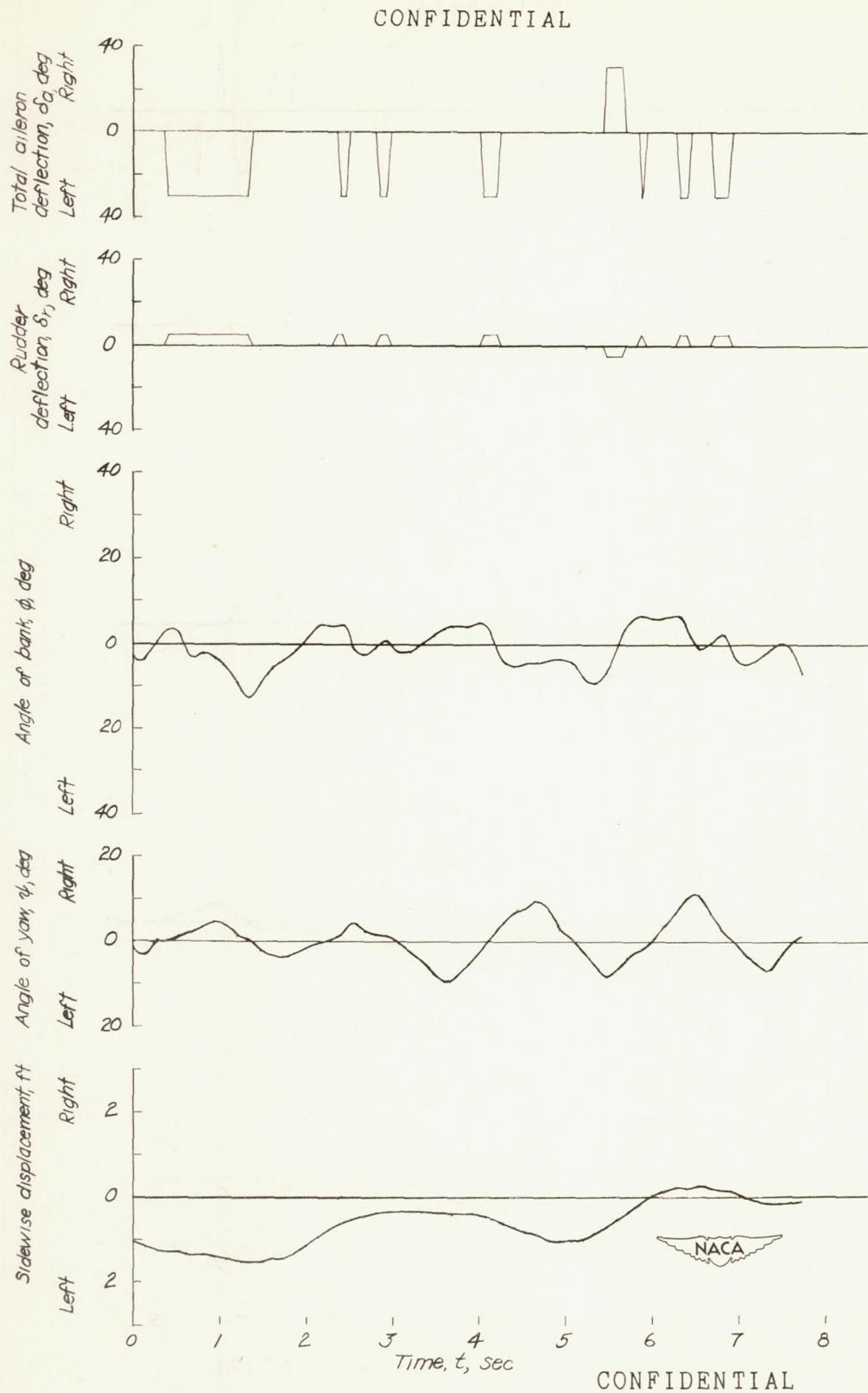
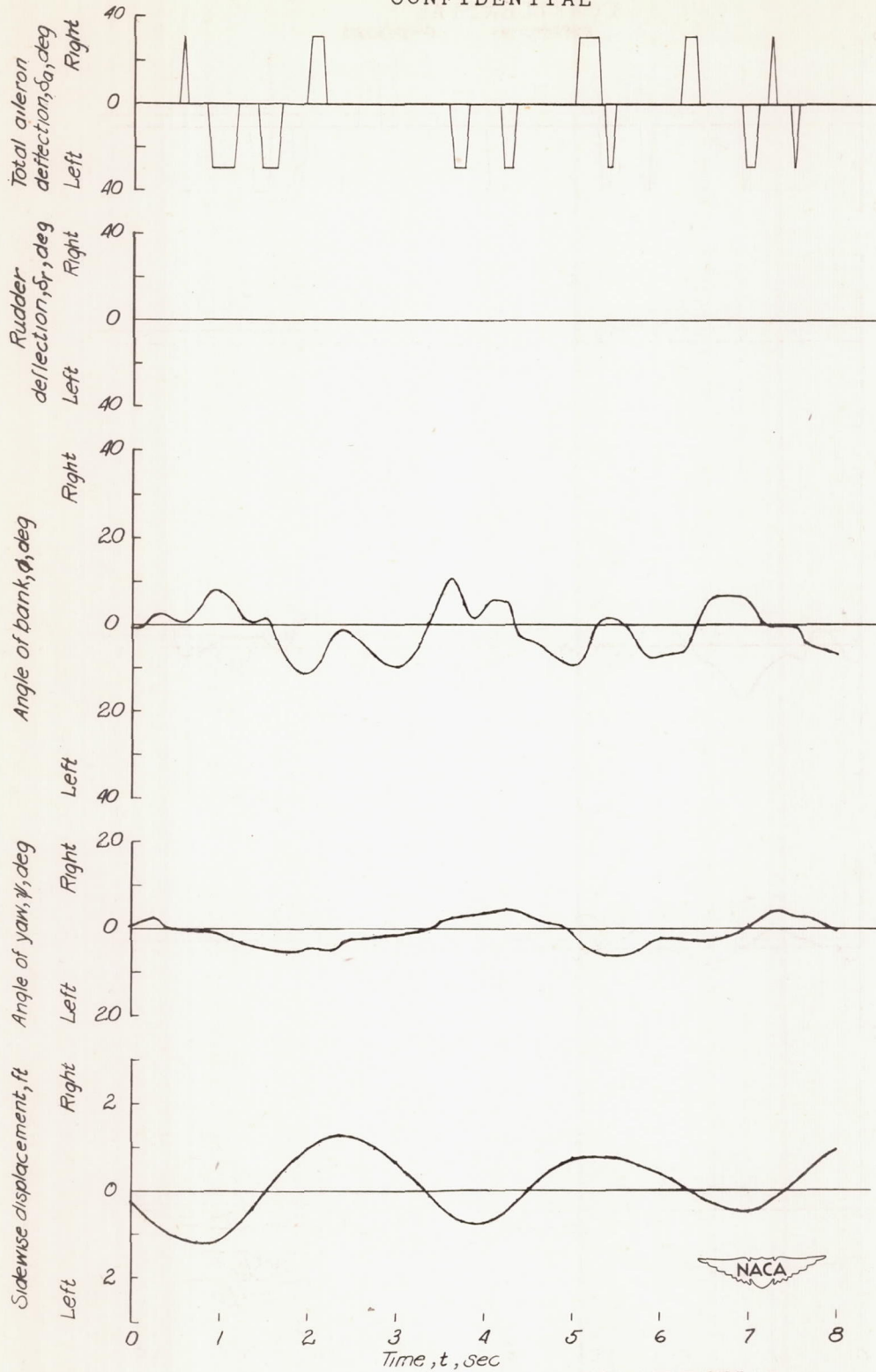


Figure 10.- Typical flight record of the lateral motions of the model for test 2 (right rudder fixed, left rudder moved 5° opposite to aileron movement, $\tau = 42^\circ$).

CONFIDENTIAL



CONFIDENTIAL

Figure 11.- Typical flight record of the lateral motions of the model for test 3 (both rudders fixed, $\tau = 42^\circ$).

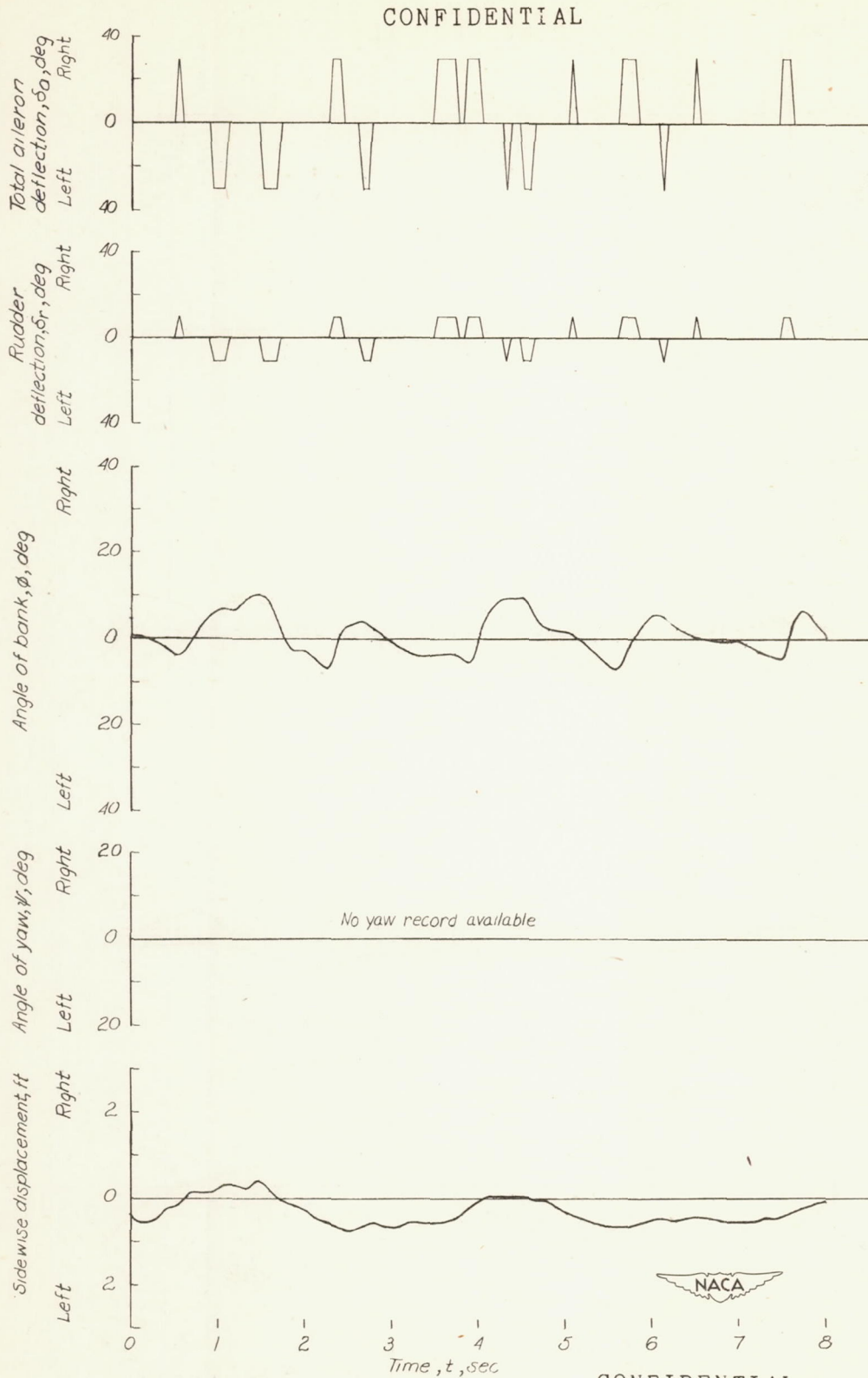


Figure 12.- Typical flight record of the lateral motions of the model for test 4 (right rudder fixed, left rudder moved 10° in the direction of aileron movement, $\tau = 42^\circ$).

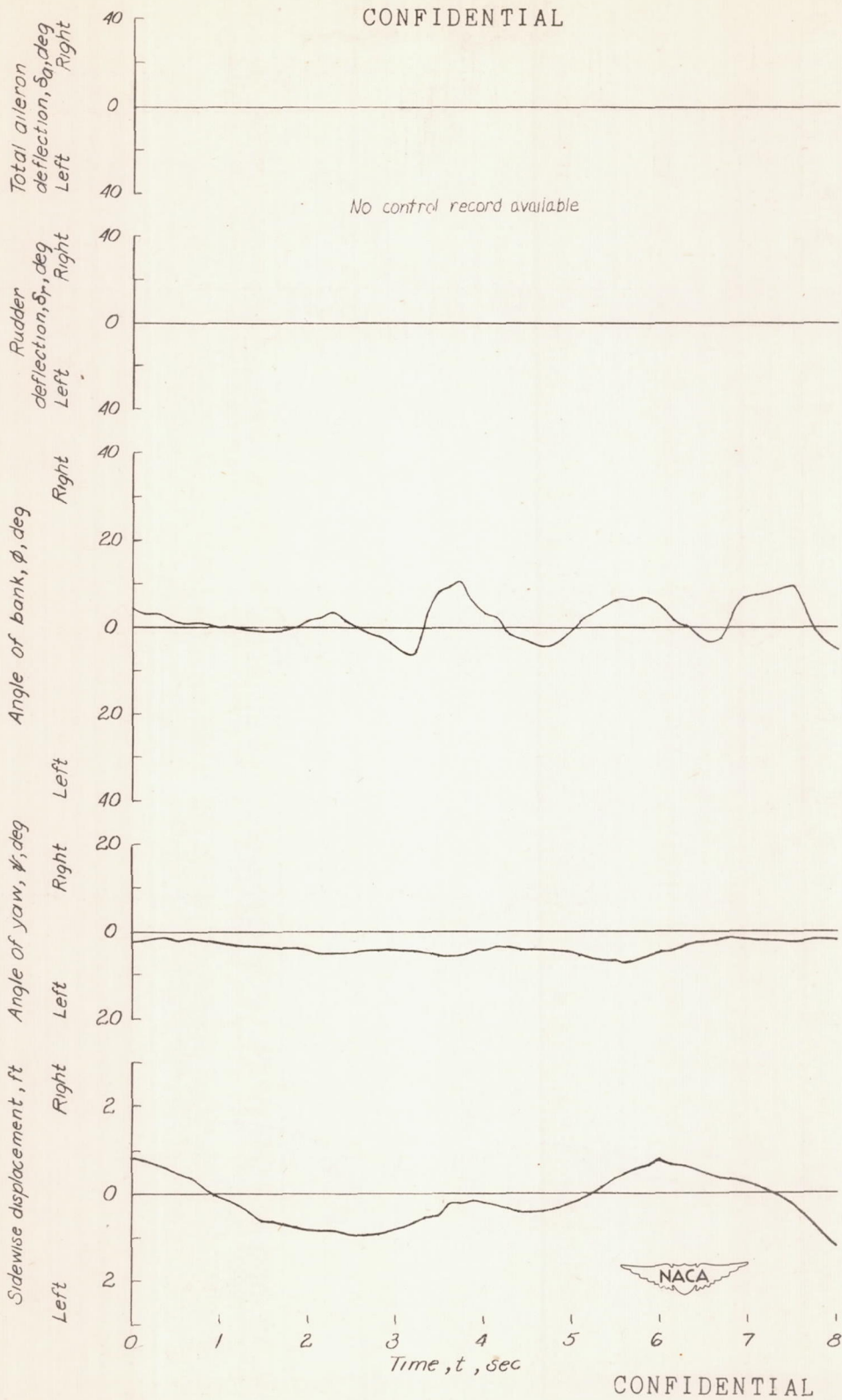
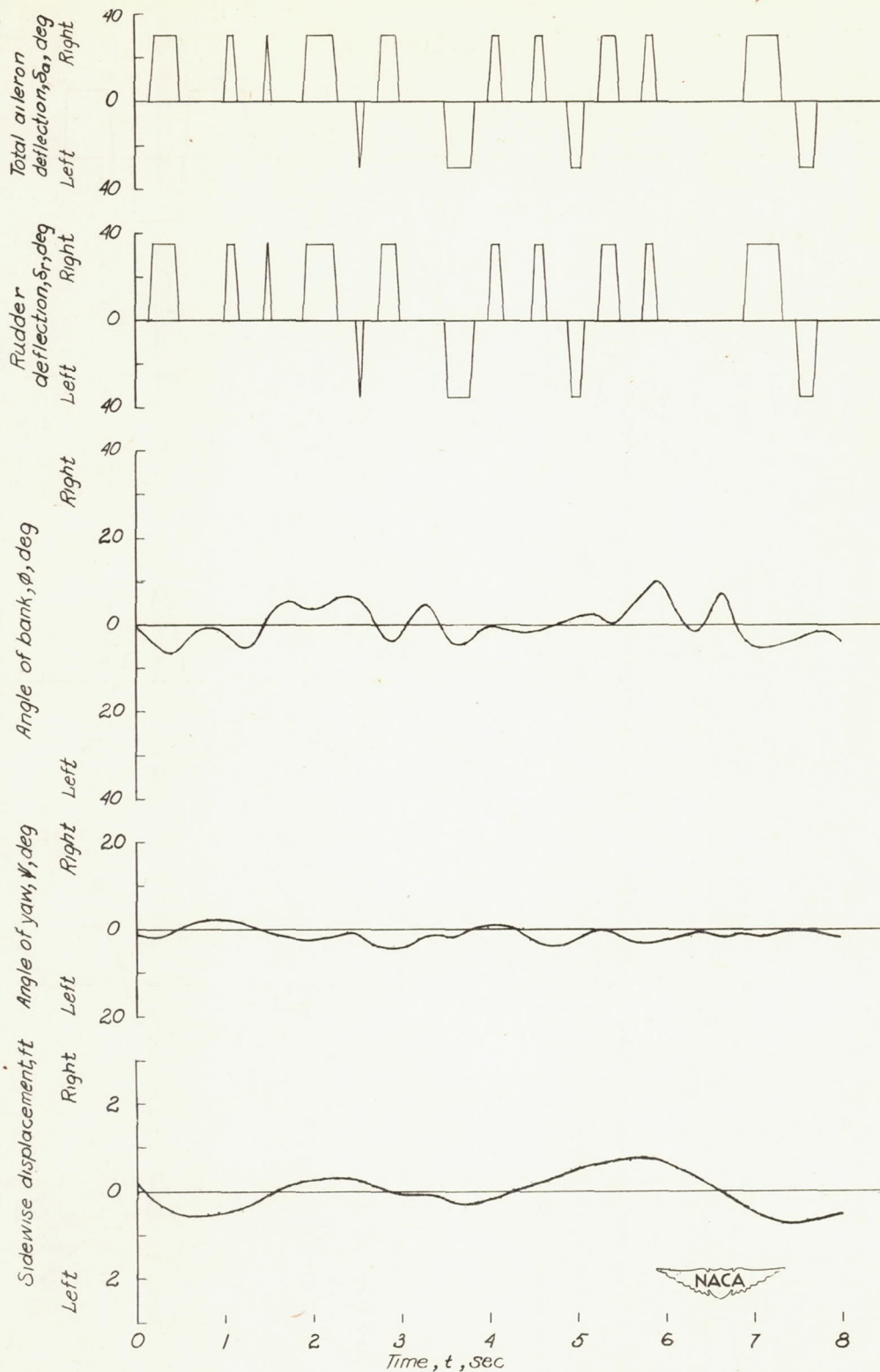


Figure 13.- Typical flight record of the lateral motions of the model for test 5 (right rudder fixed, left rudder moved 20° in the direction of aileron movement, $\tau = 42^\circ$).

CONFIDENTIAL



CONFIDENTIAL

Figure 14.- Typical flight record of the lateral motions of the model for test 6 (right rudder fixed, left rudder moved 35° in the direction of aileron movement, $\tau = 42^\circ$).

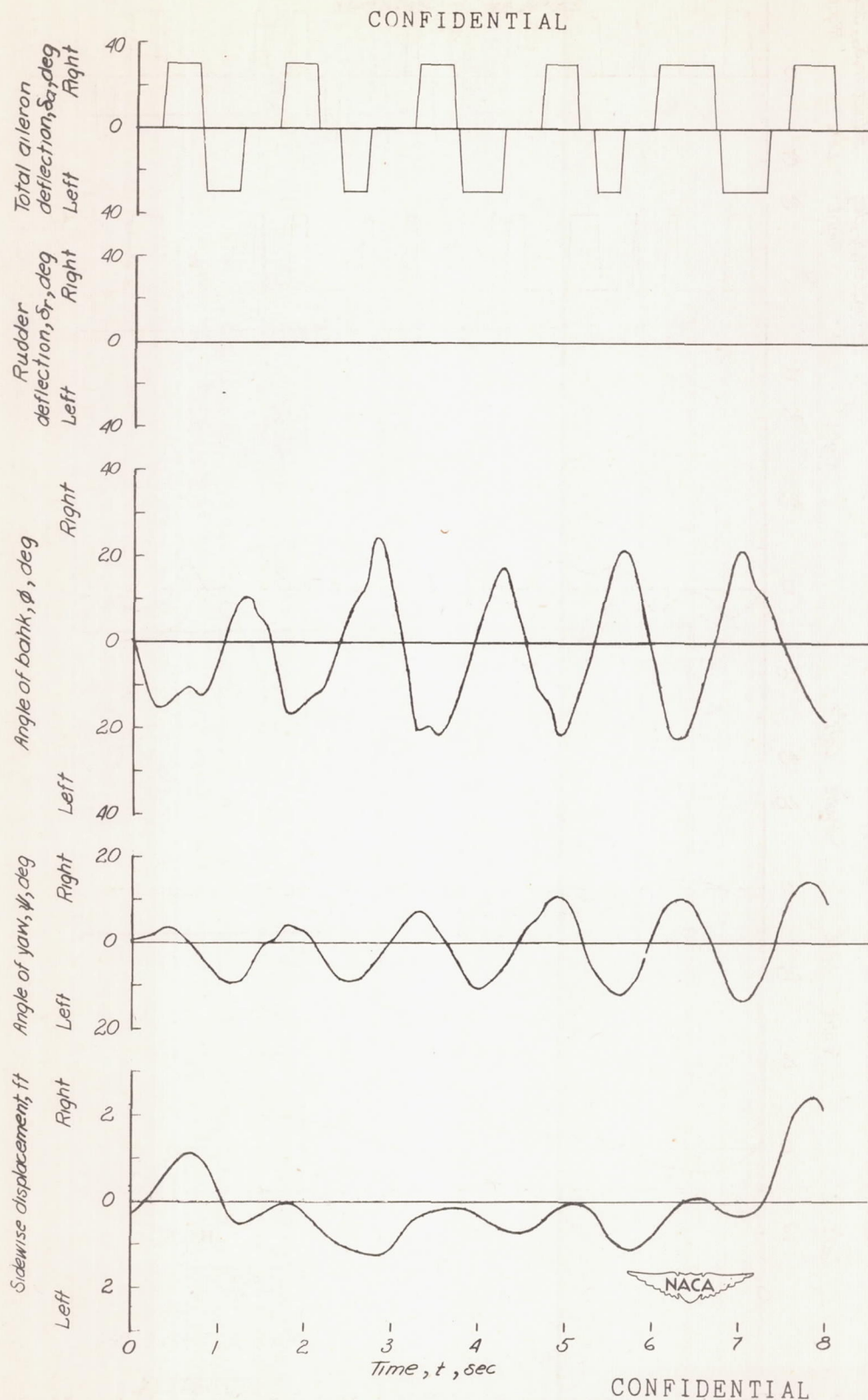
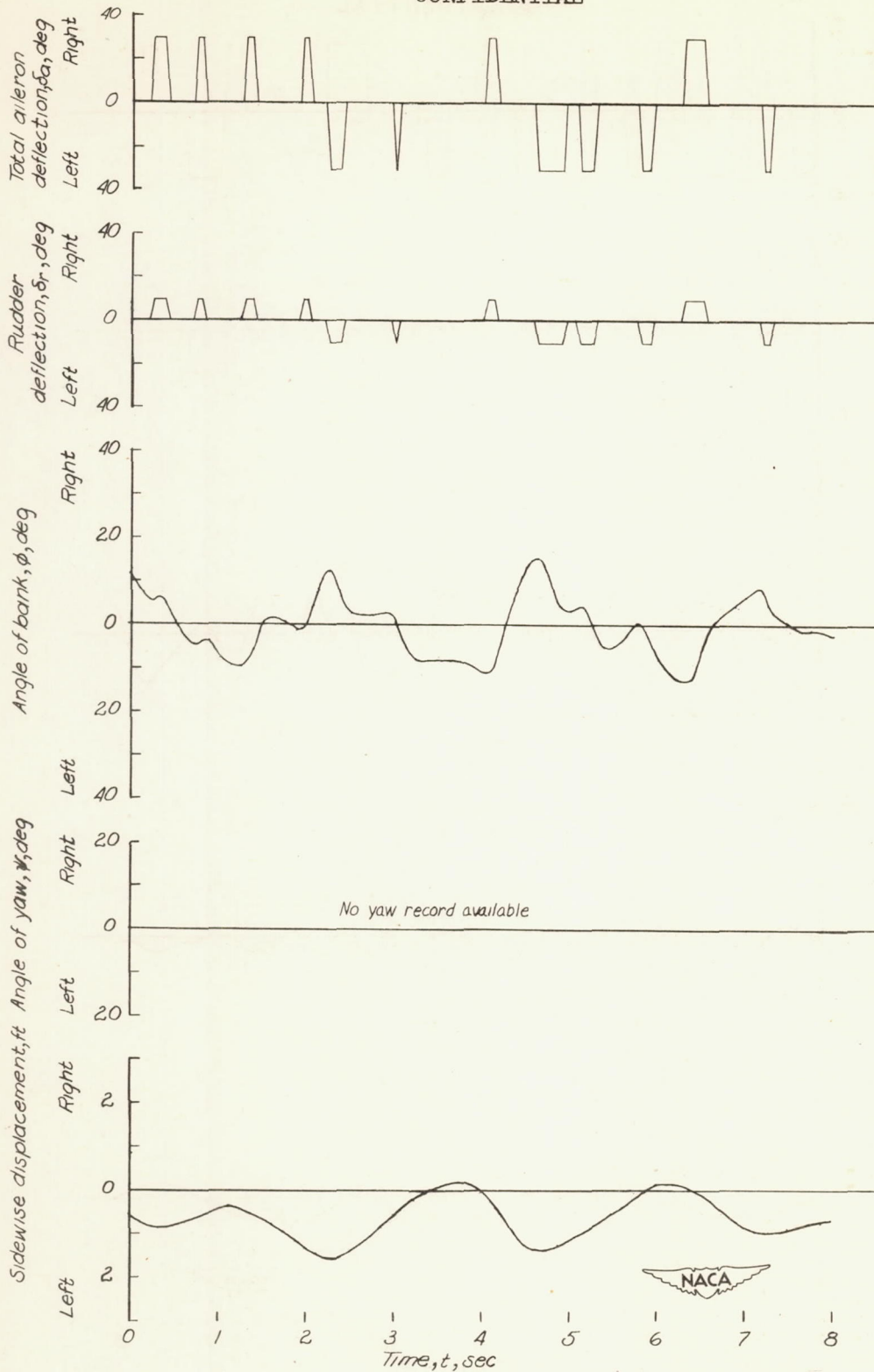


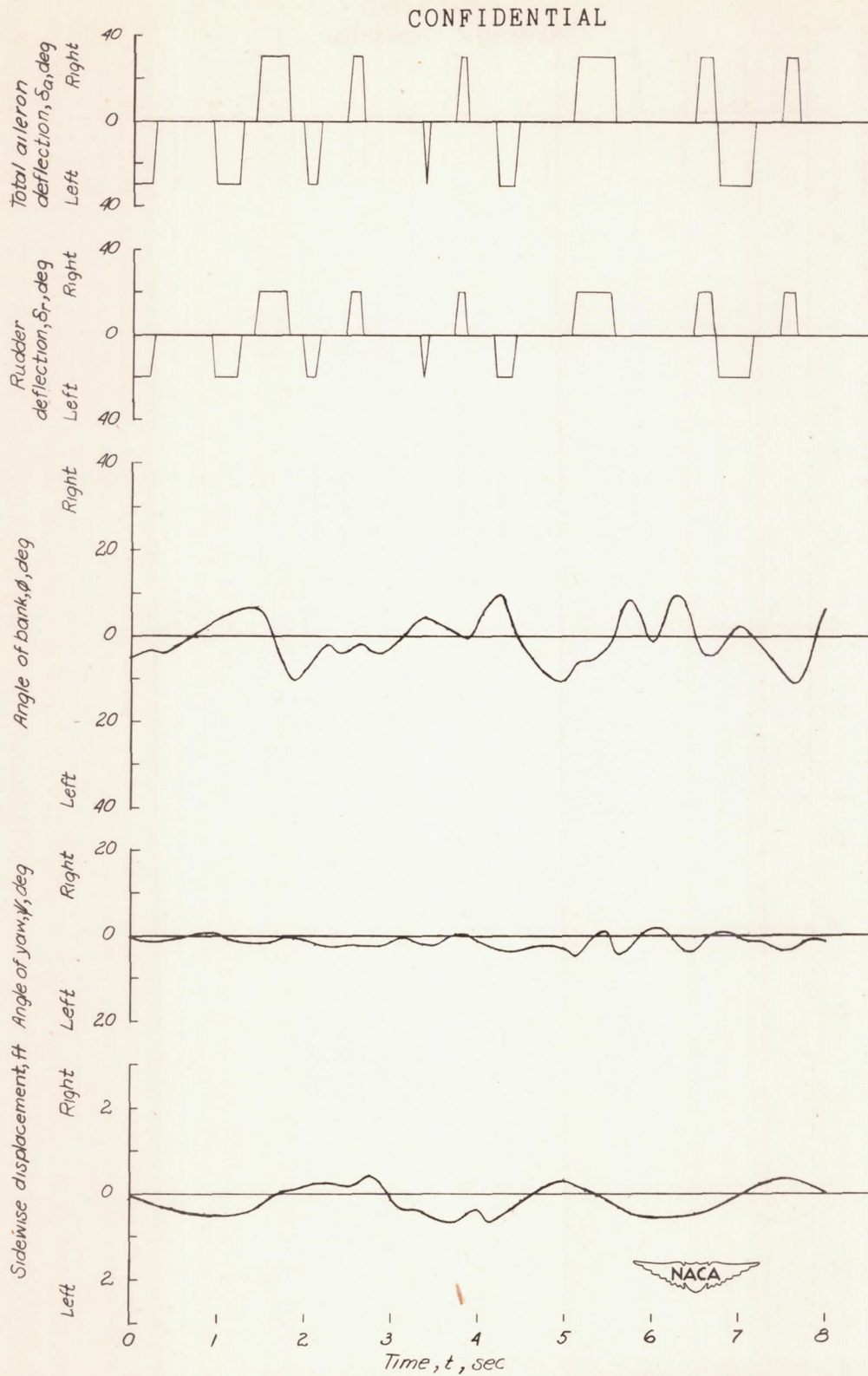
Figure 15.- Typical flight record of the lateral motions of the model for test 7 (both rudders fixed, $\tau = 32^\circ$).

CONFIDENTIAL



CONFIDENTIAL.

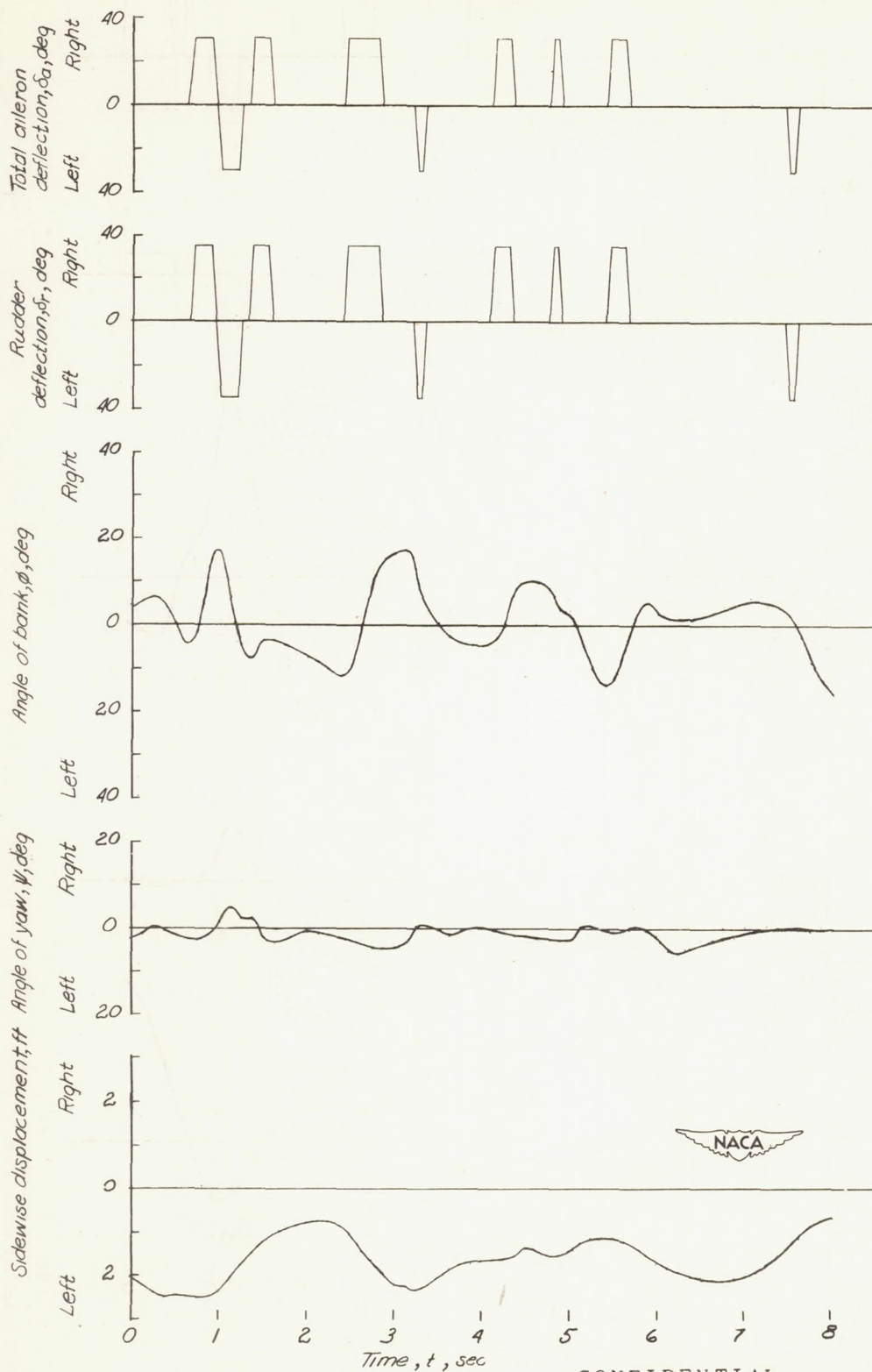
Figure 16.- Typical flight record of the lateral motions of the model for test 8 (right rudder fixed, left rudder moved 10° in the direction of aileron movement, $\tau = 32^\circ$).



CONFIDENTIAL

Figure 17.- Typical flight record of the lateral motions of the model for test 9 (right rudder fixed, left rudder moved 20° in the direction of aileron movement, $\tau = 32^\circ$).

CONFIDENTIAL



CONFIDENTIAL

Figure 18.- Typical flight record of the lateral motions of the model for test 10 (right rudder fixed, left rudder moved 35° in the direction of aileron movement, $\tau = 32^\circ$).

CONFIDENTIAL

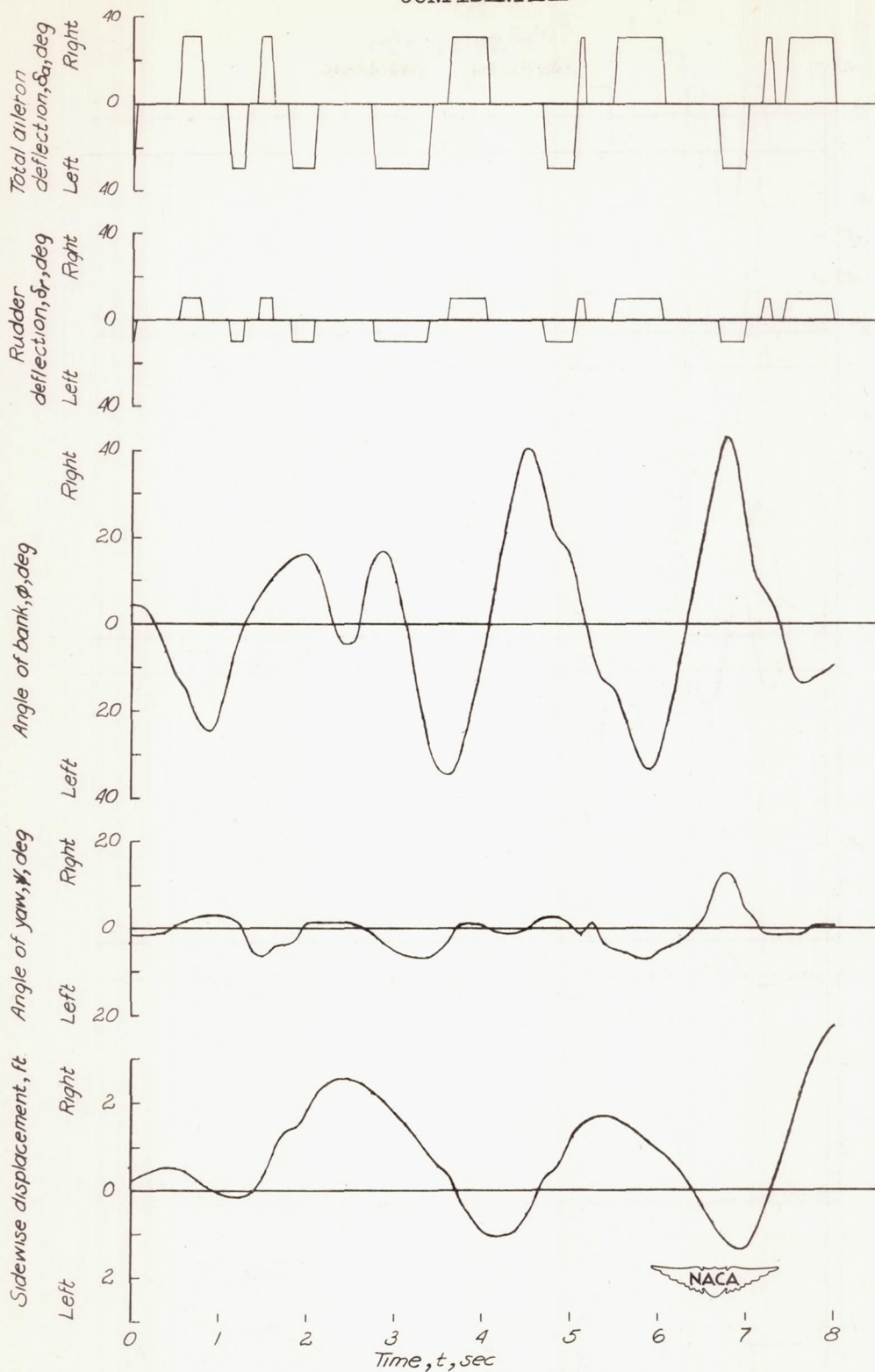


Figure 19.- Typical flight record of the lateral motions of the model for test 11 (right rudder fixed, left rudder moved 10° in the direction of aileron movement, $\tau = 26^\circ$).

CONFIDENTIAL

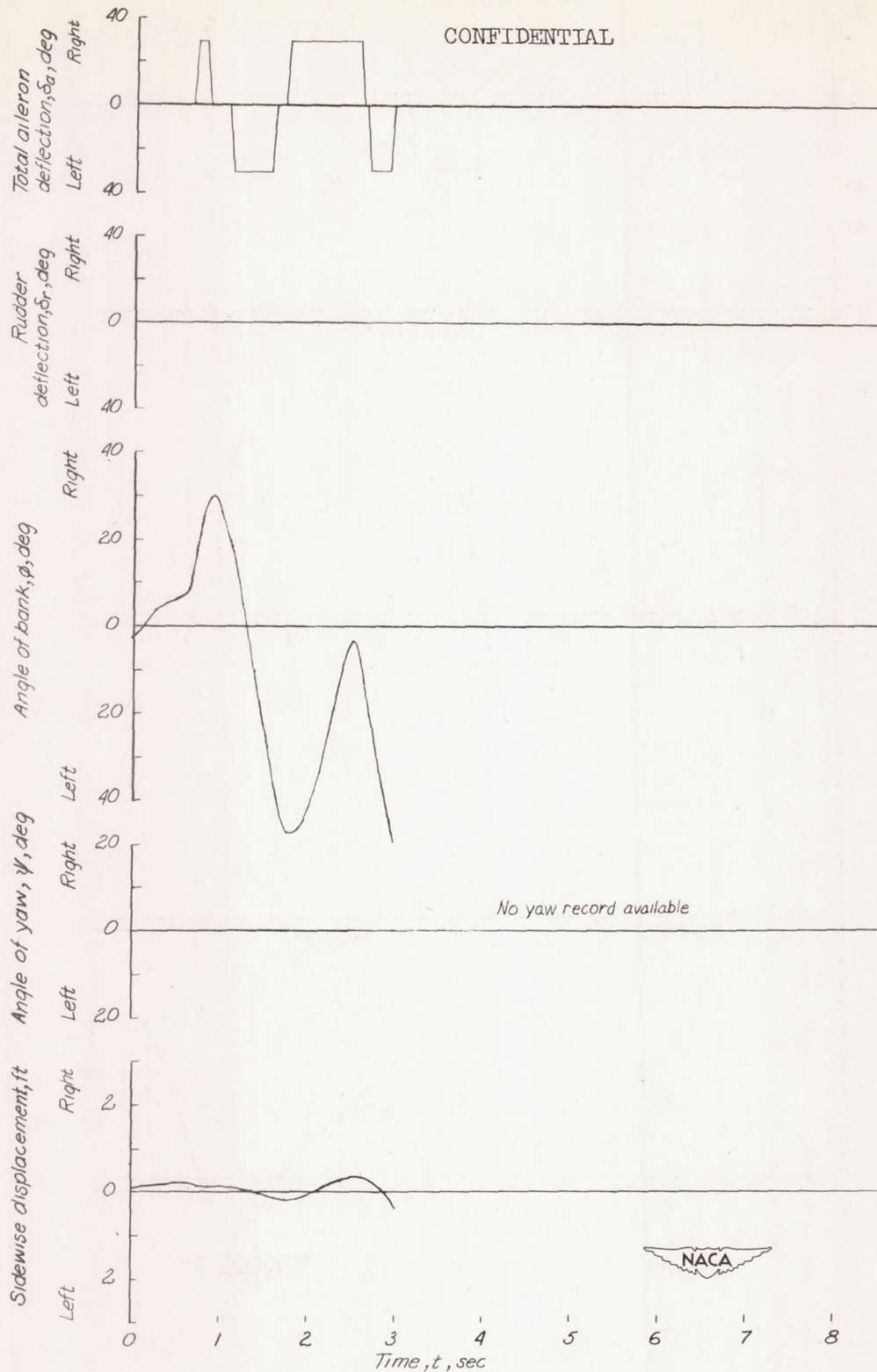
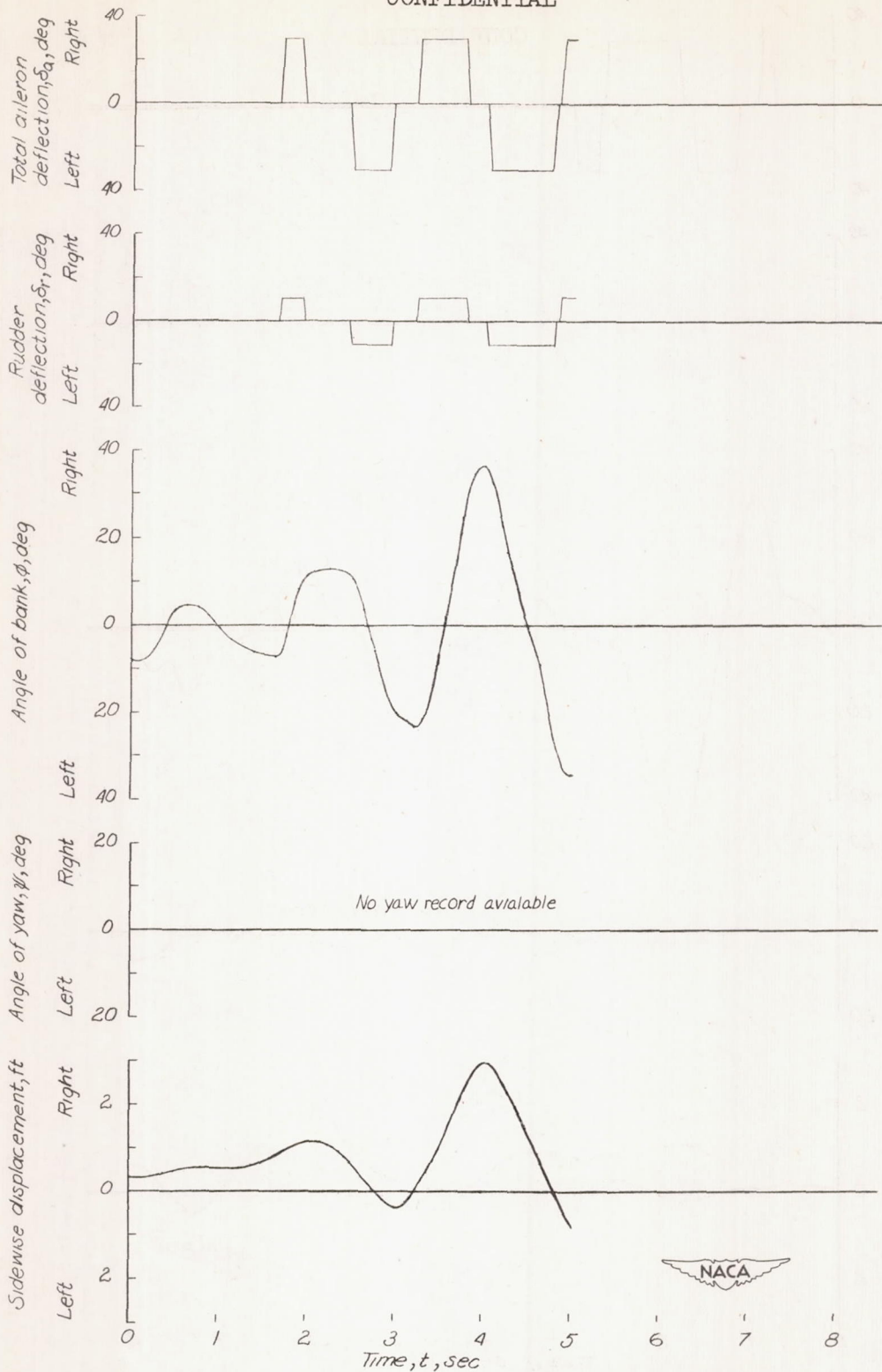


Figure 20.- Typical flight record of the lateral motions of the model for test 12 (both rudders fixed, $\tau = 20^\circ$).

CONFIDENTIAL



CONFIDENTIAL

Figure 21 - Typical flight record of the lateral motions of the model for test 13 (right rudder fixed, left rudder moved 10° in the direction of aileron movement, $\tau = 20^\circ$).

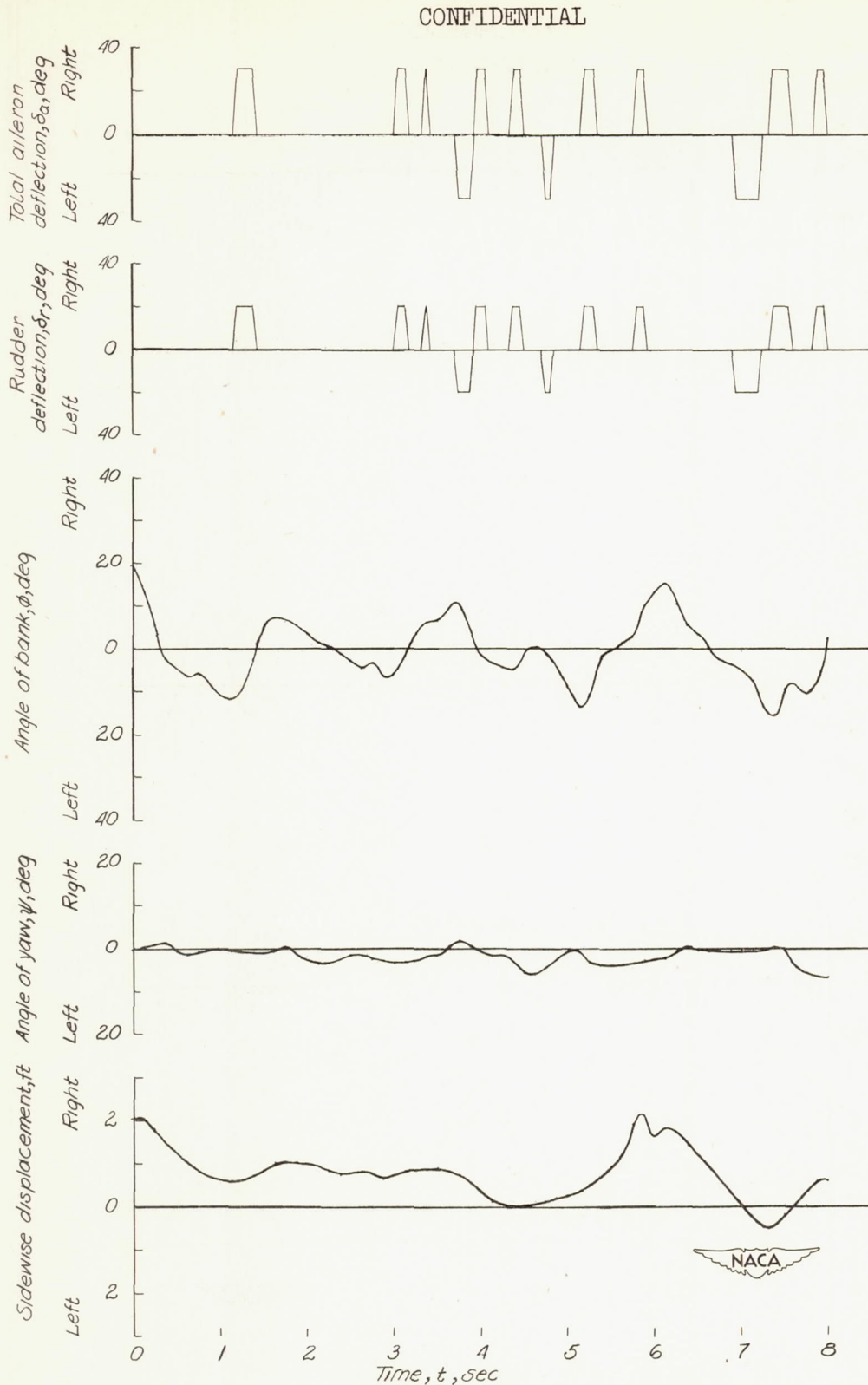
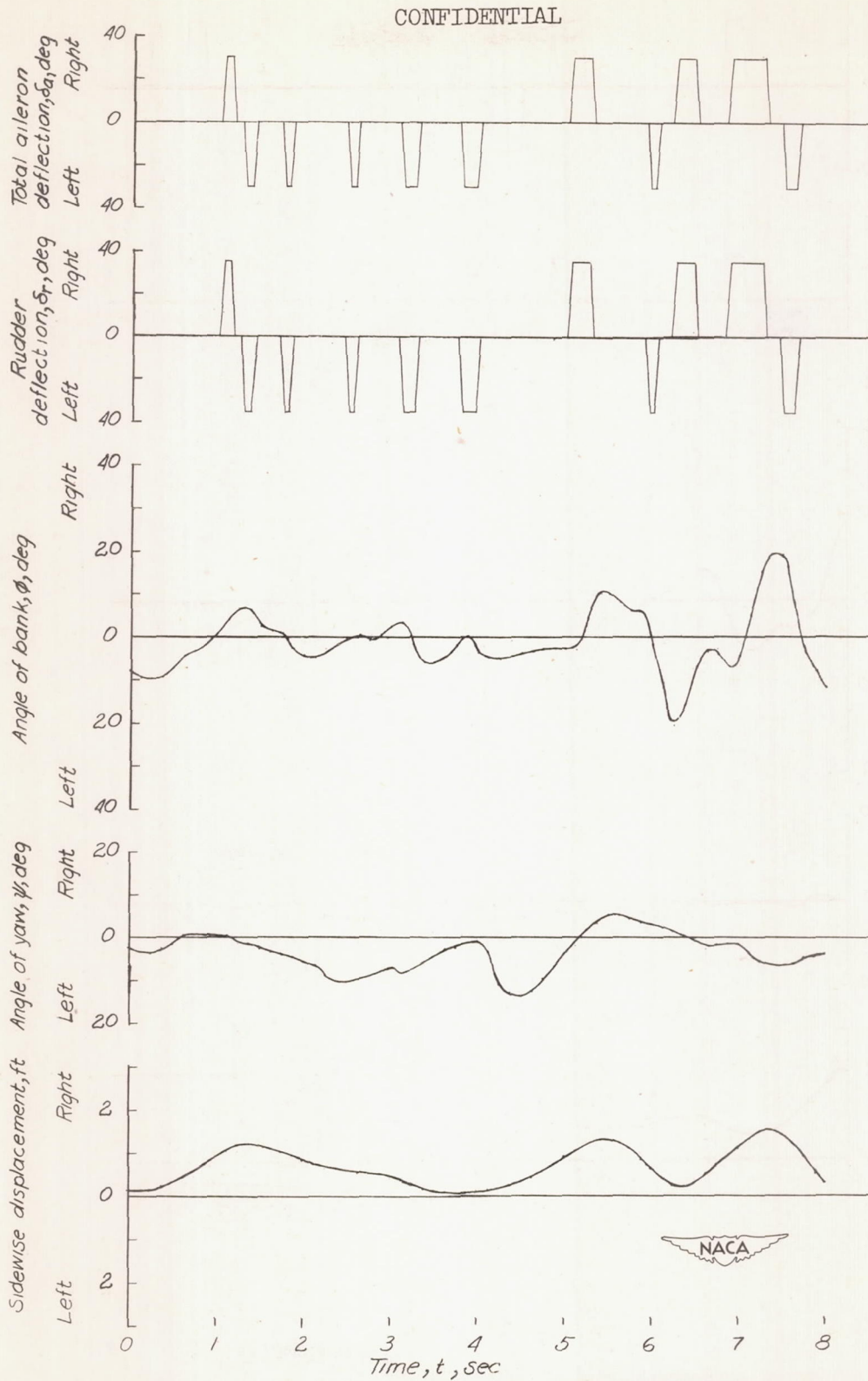


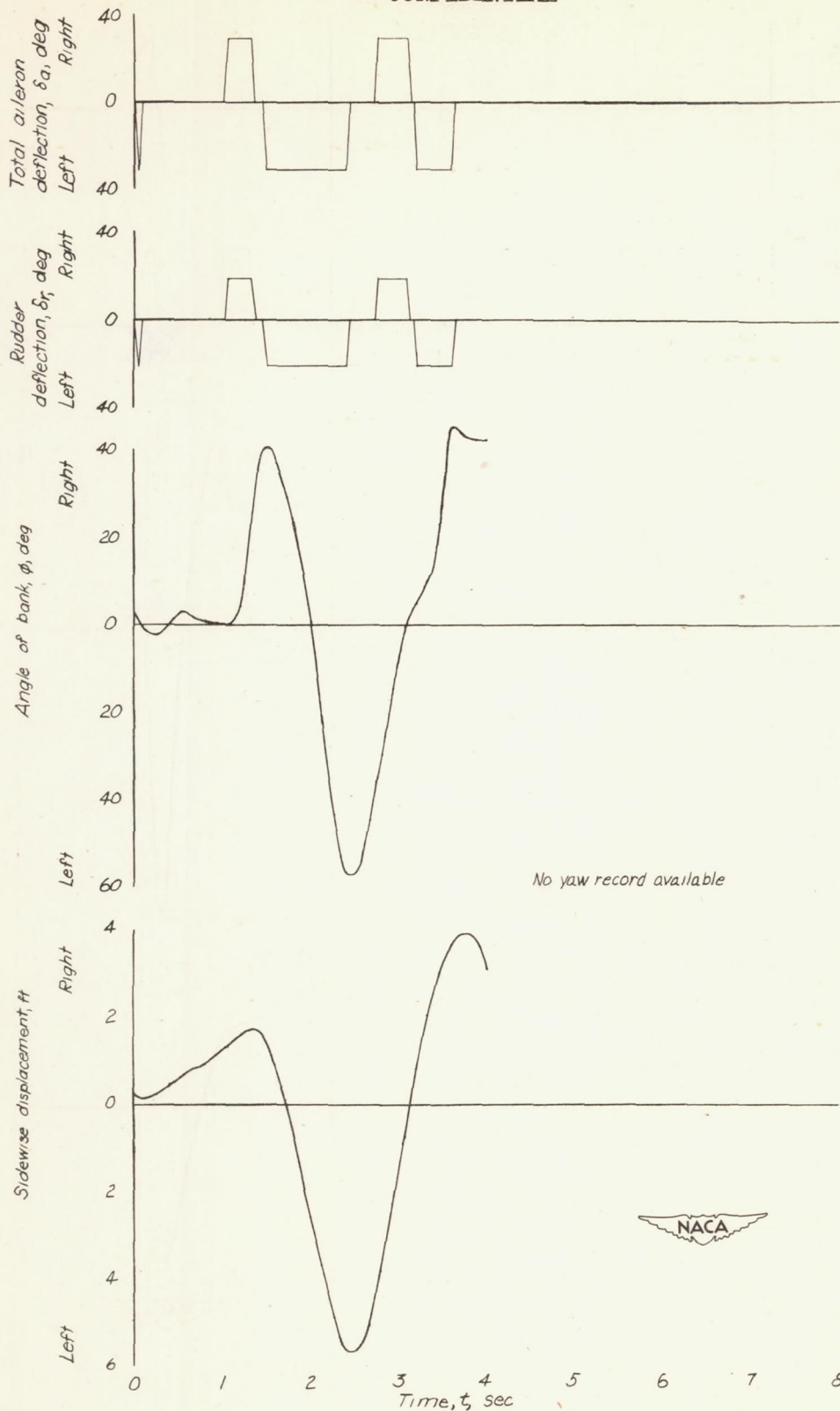
Figure 22.- Typical flight record of the lateral motions of the model for test 14 (right rudder fixed, left rudder moved 25° in the direction of aileron movement, $\tau = 20^\circ$).



CONFIDENTIAL

Figure 23.- Typical flight record of the lateral motions of the model for test 15 (right rudder fixed, left rudder moved 35° in the direction of aileron movement, $\tau = 20^\circ$).

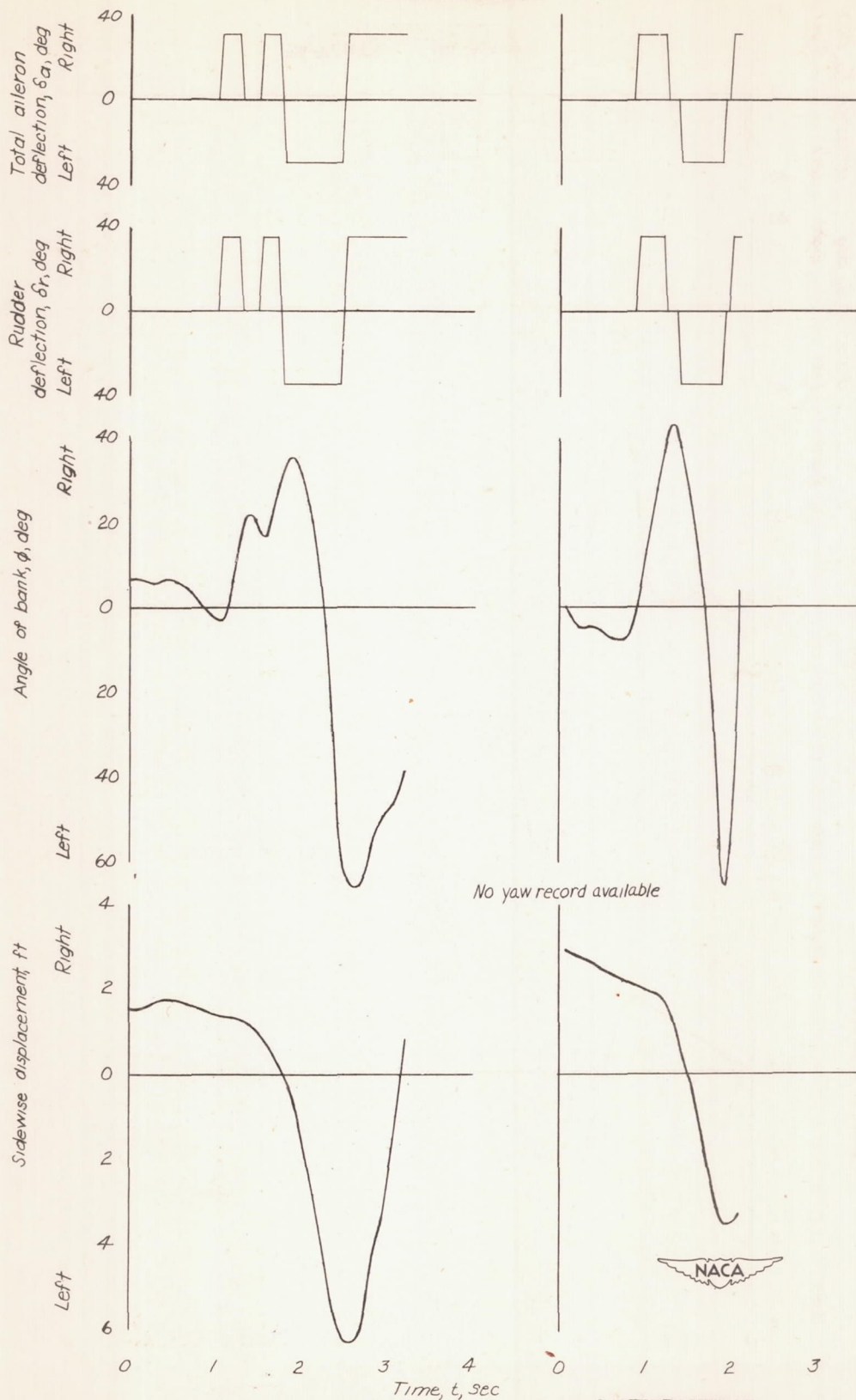
CONFIDENTIAL



CONFIDENTIAL

Figure 24.- Typical flight record of the lateral motions of the model for test 16 (both rudders moved 20° in the direction of aileron movement, $\tau = 8^\circ$).

CONFIDENTIAL



CONFIDENTIAL

Figure 25.- Typical flight record of the lateral motions of the model for test 17 (both rudders moved 35° in the direction of aileron movement, $\tau = 8^\circ$).

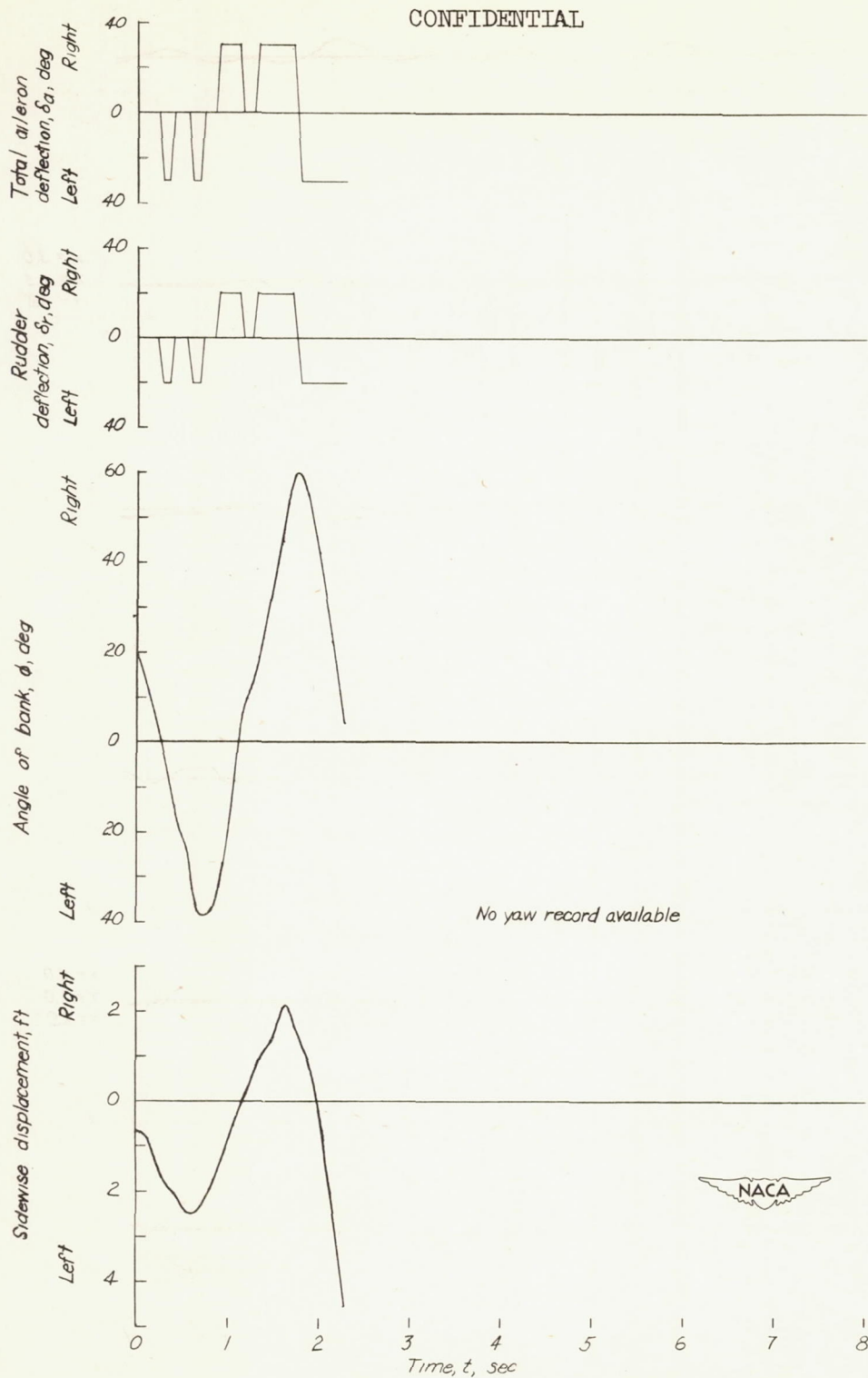
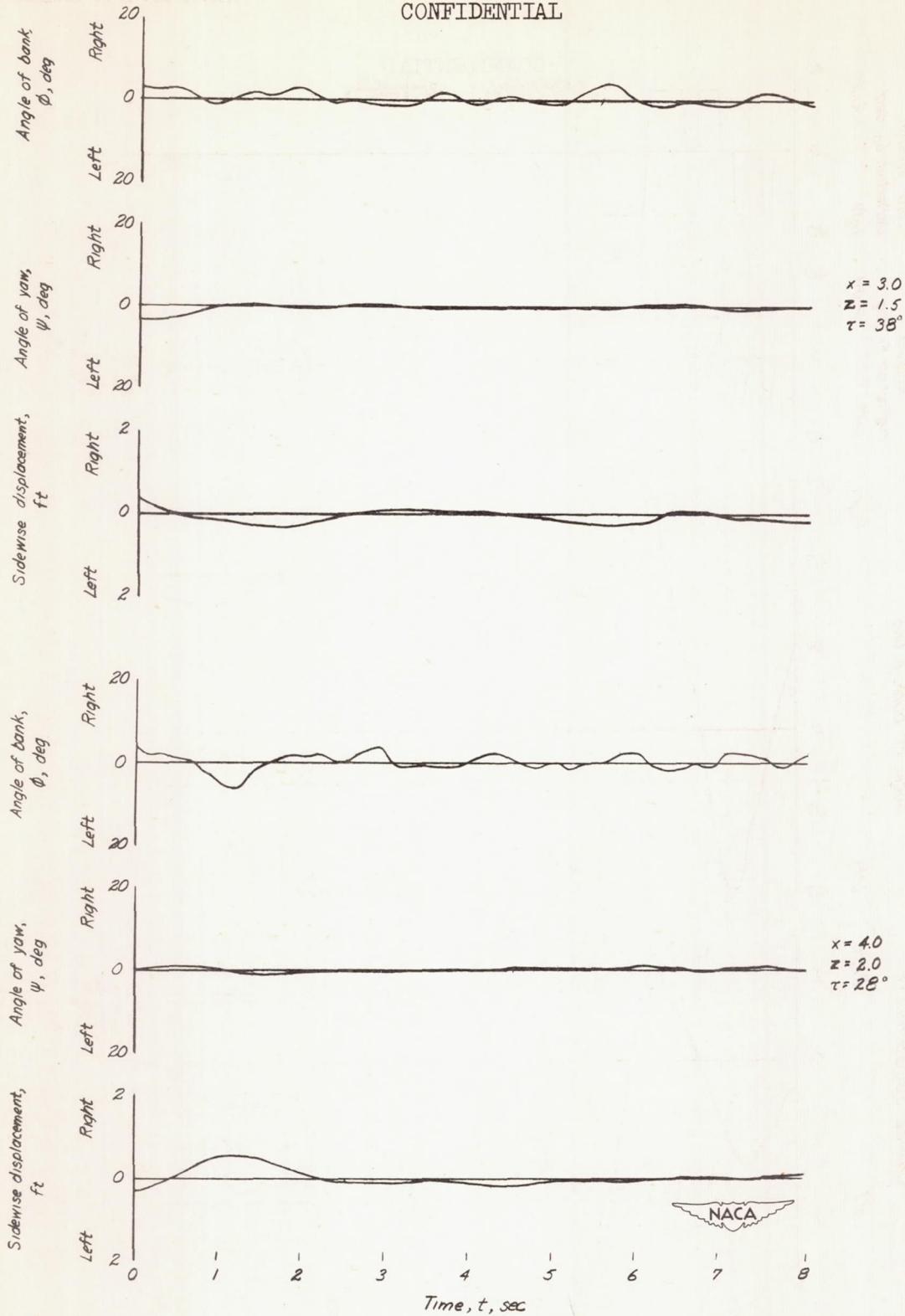


Figure 26.- Typical flight record of the lateral motions of the model for test 18 (both rudders moved 20° in the direction of aileron movement, $\tau = 0^\circ$).

CONFIDENTIAL

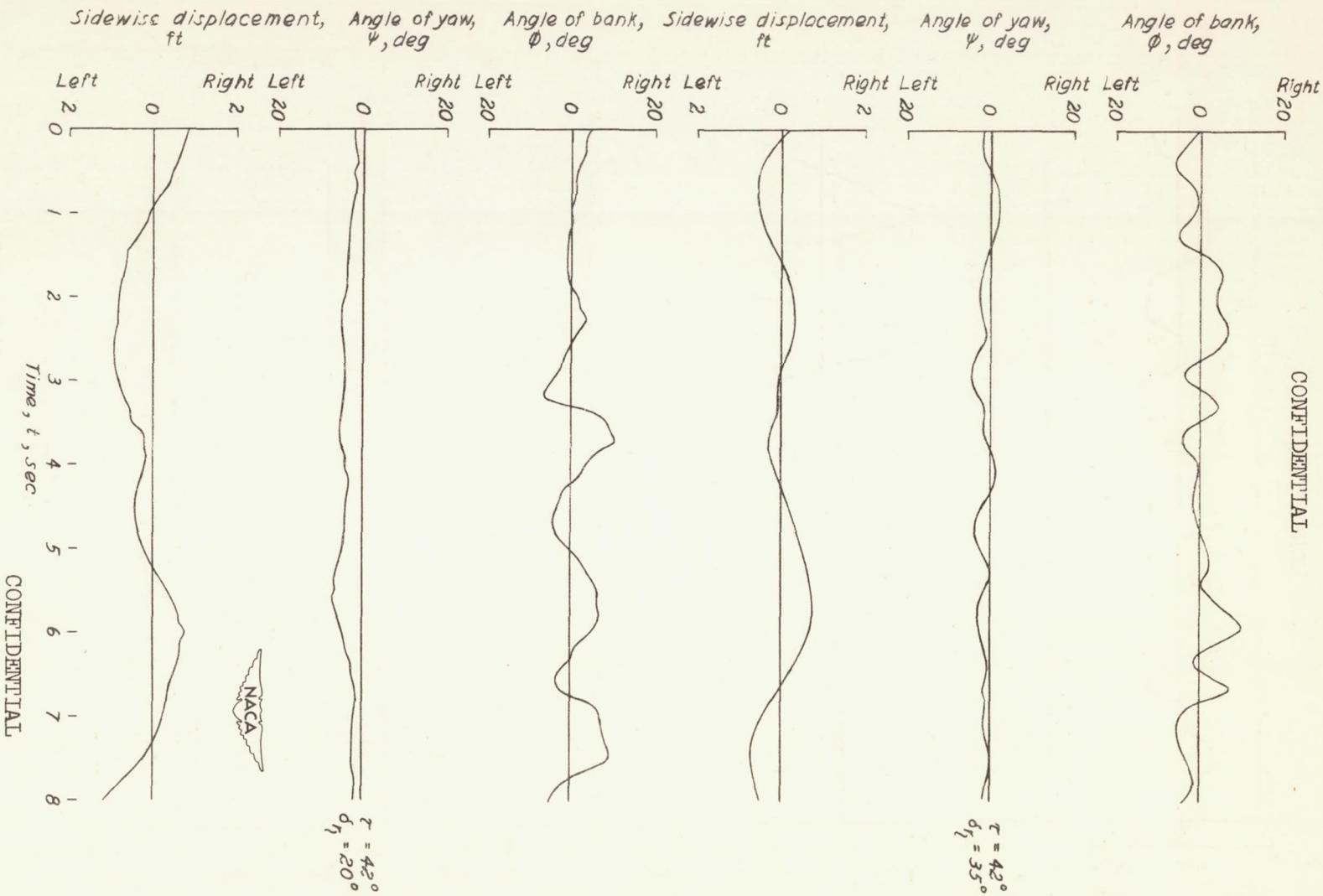


CONFIDENTIAL

(a) Proportional control.

Figure 27.- Comparison of the lateral motions of the model with proportional and flicker control systems in the two best conditions covered in the tests of each control system.

CONFIDENTIAL



CONFIDENTIAL

(b) Flicker control.

Figure 27.- Concluded.

CONFIDENTIAL

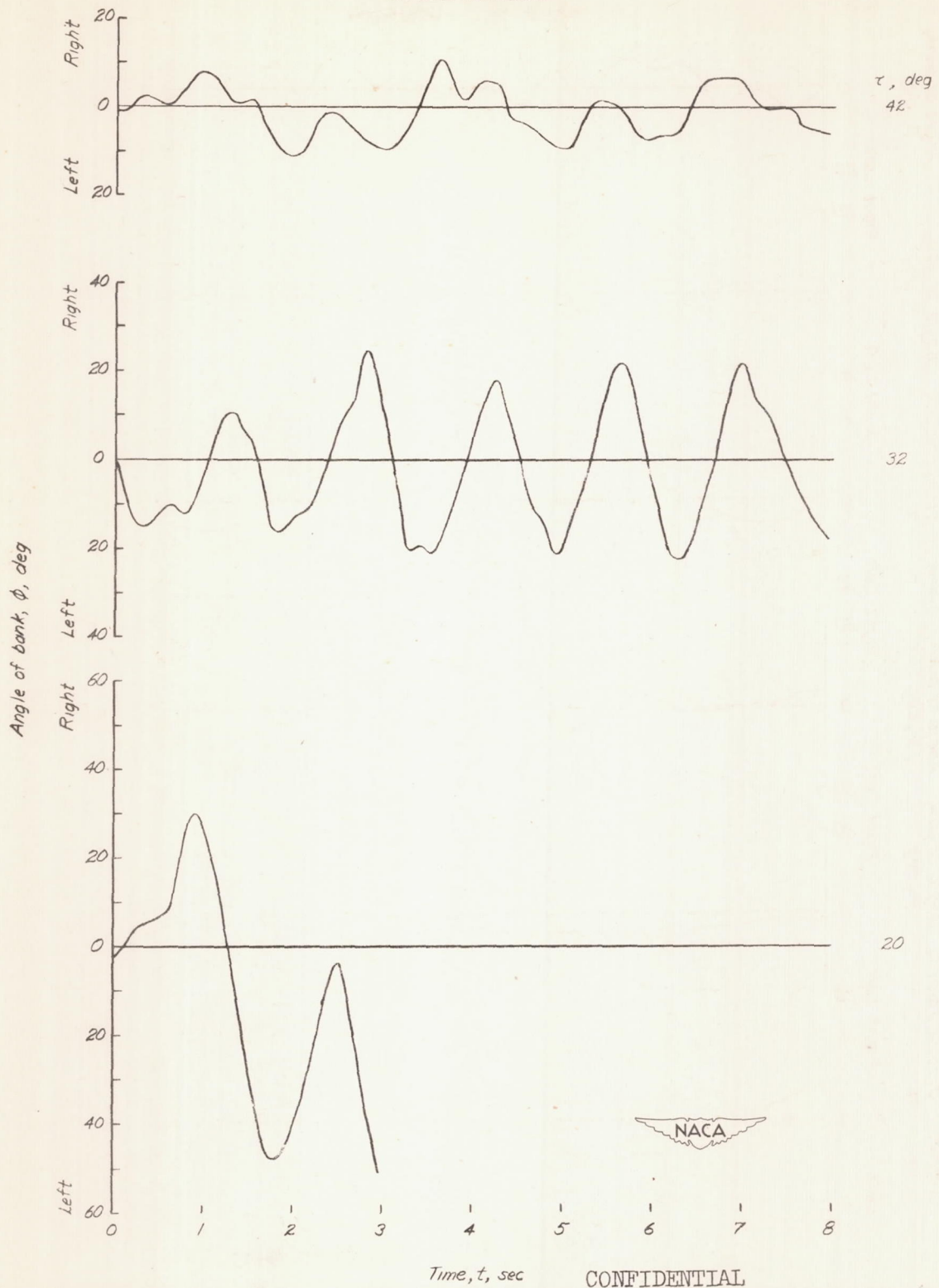


Figure 28.- Typical flight records of the rolling motions of the model showing the effect of varying the angle of tilt τ , both rudders fixed.

CONFIDENTIAL

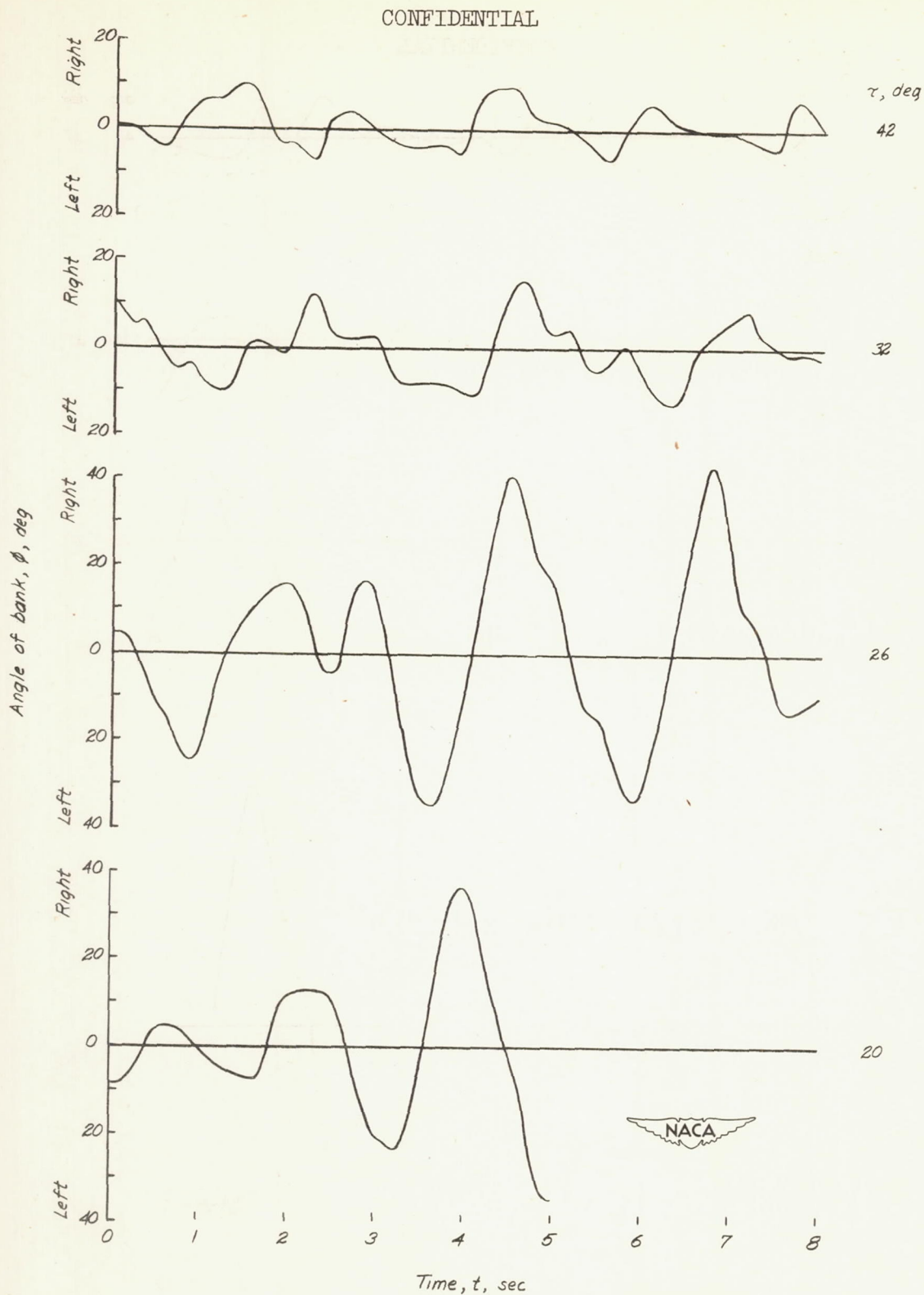


Figure 29.- Typical flight records of the rolling motions of the model showing the effect of varying the angle of tilt τ , right rudder fixed, left rudder moved 10° in the direction of the aileron movement.

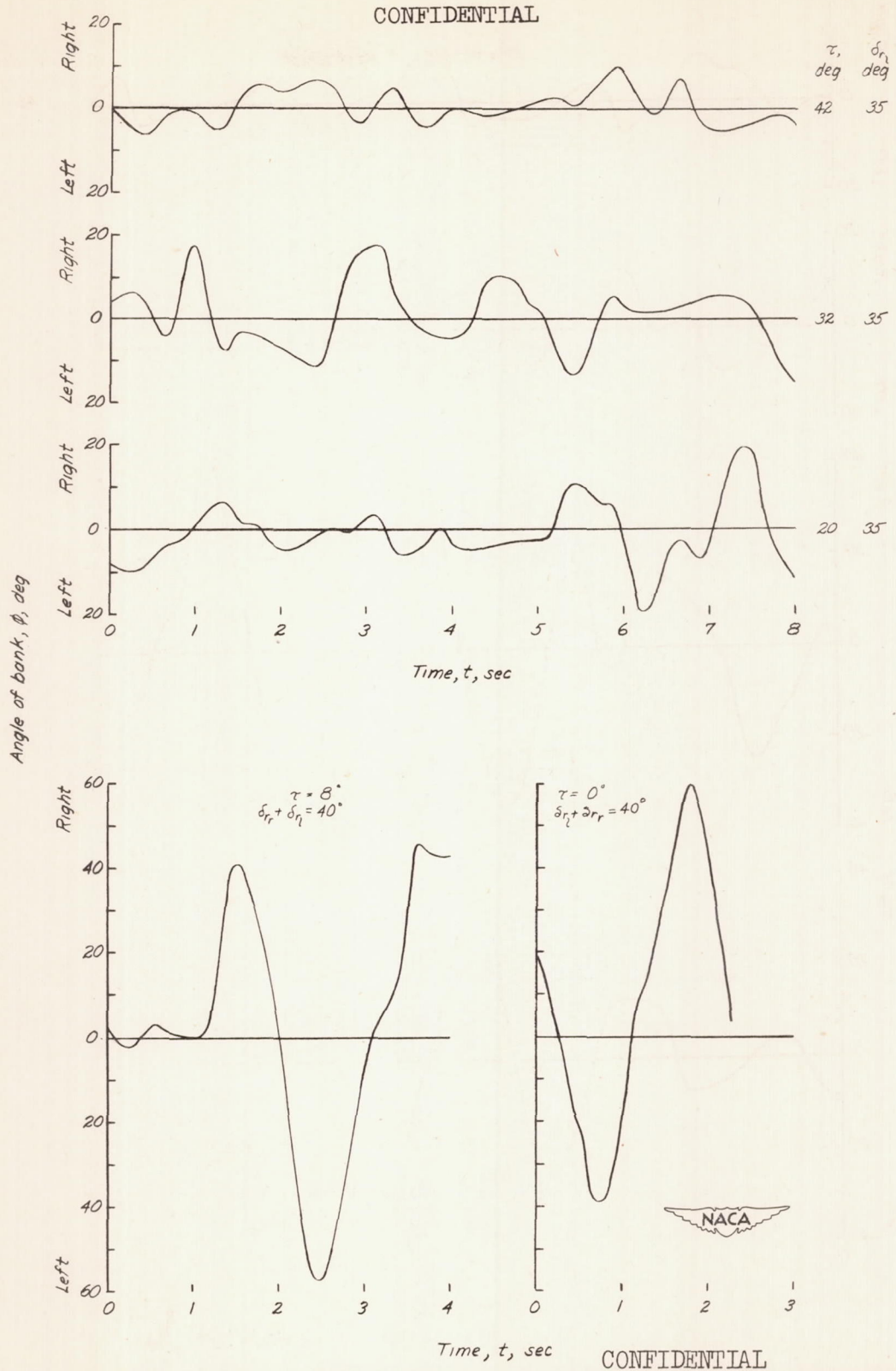


Figure 30.- Typical flight record of the rolling motions of the model showing the effect of varying the angle of tilt τ .

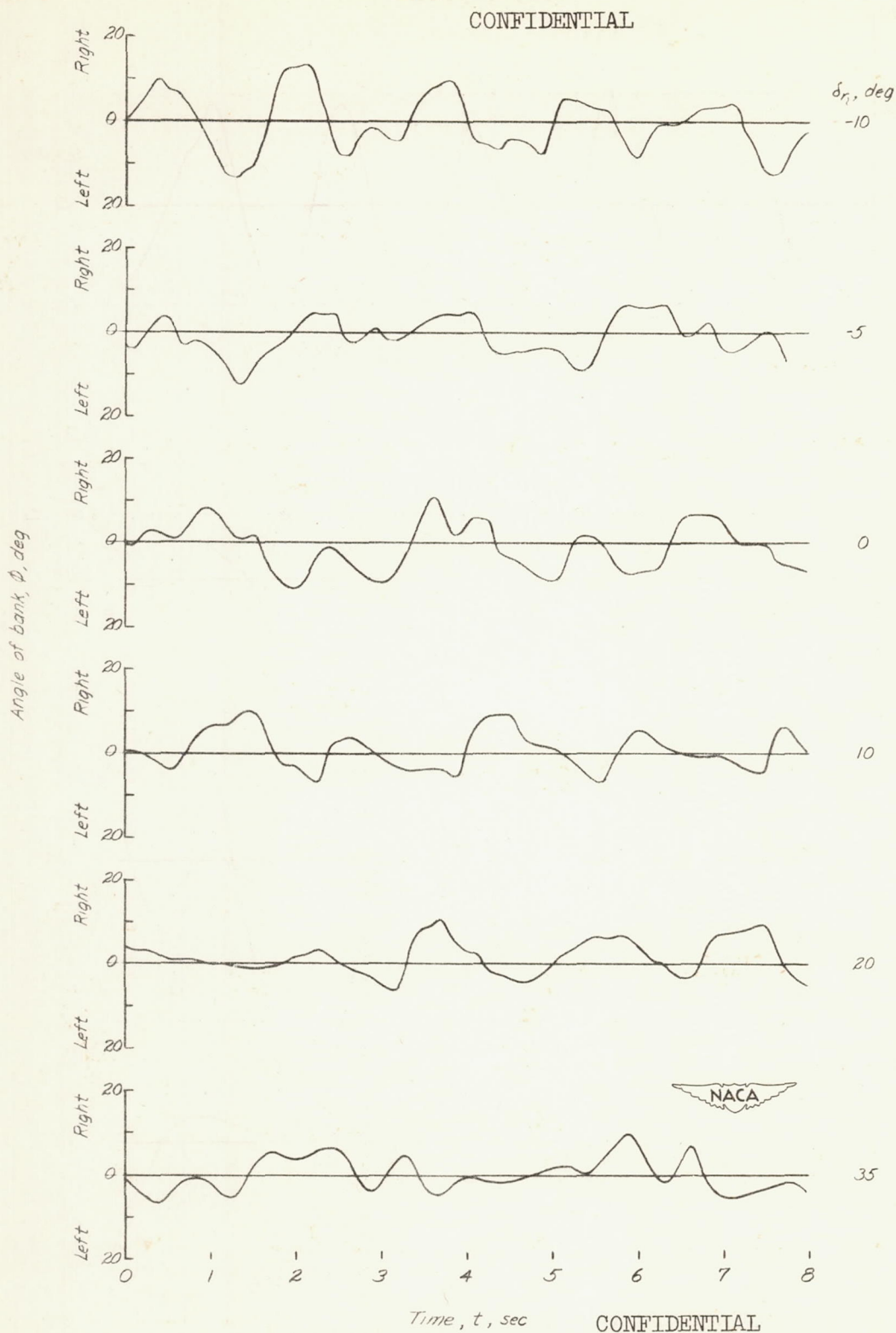
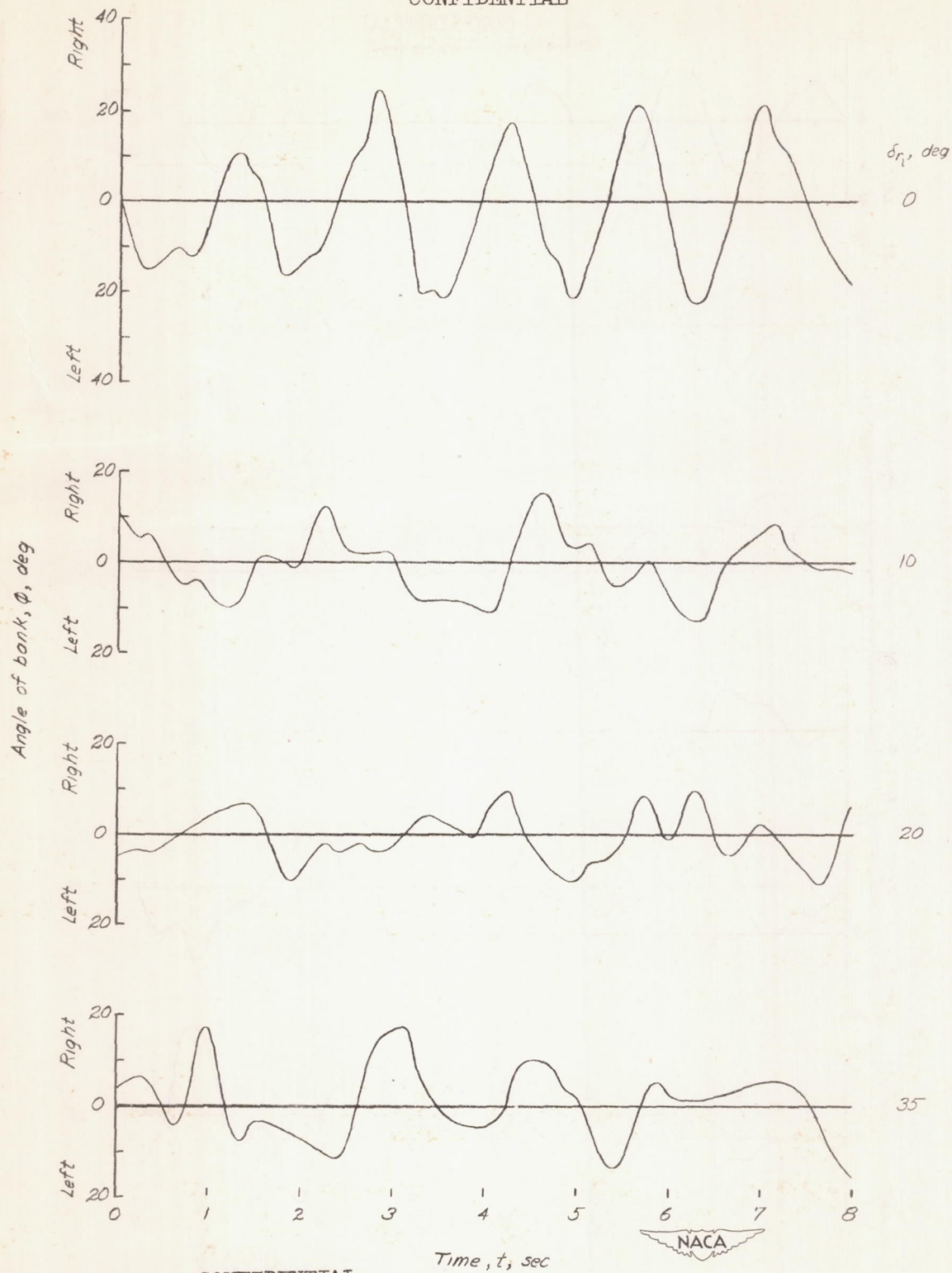


Figure 31.- Typical flight records of the rolling motions of the model showing the effect of varying the ratio of rudder deflection to aileron deflection, $\tau = 42^\circ$.

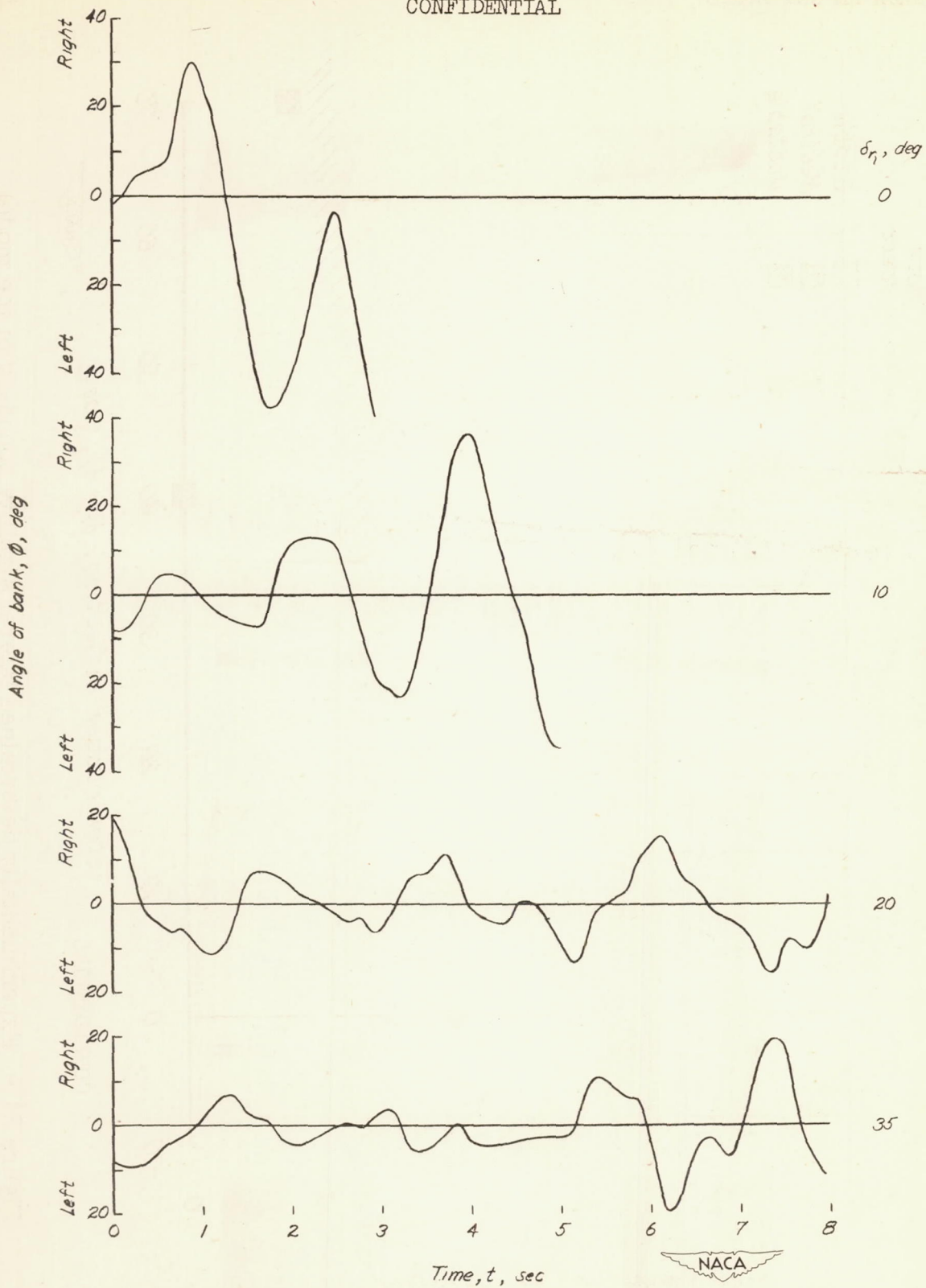
CONFIDENTIAL



CONFIDENTIAL

Figure 32.- Typical flight records of the rolling motions of the model showing the effect of varying the ratio of rudder deflection to aileron deflection, $\tau = 32^\circ$.

CONFIDENTIAL



CONFIDENTIAL

Figure 33.- Typical flight records of the rolling motions of the model showing the effect of varying the ratio of rudder deflection to aileron deflection, $\tau = 20^\circ$.

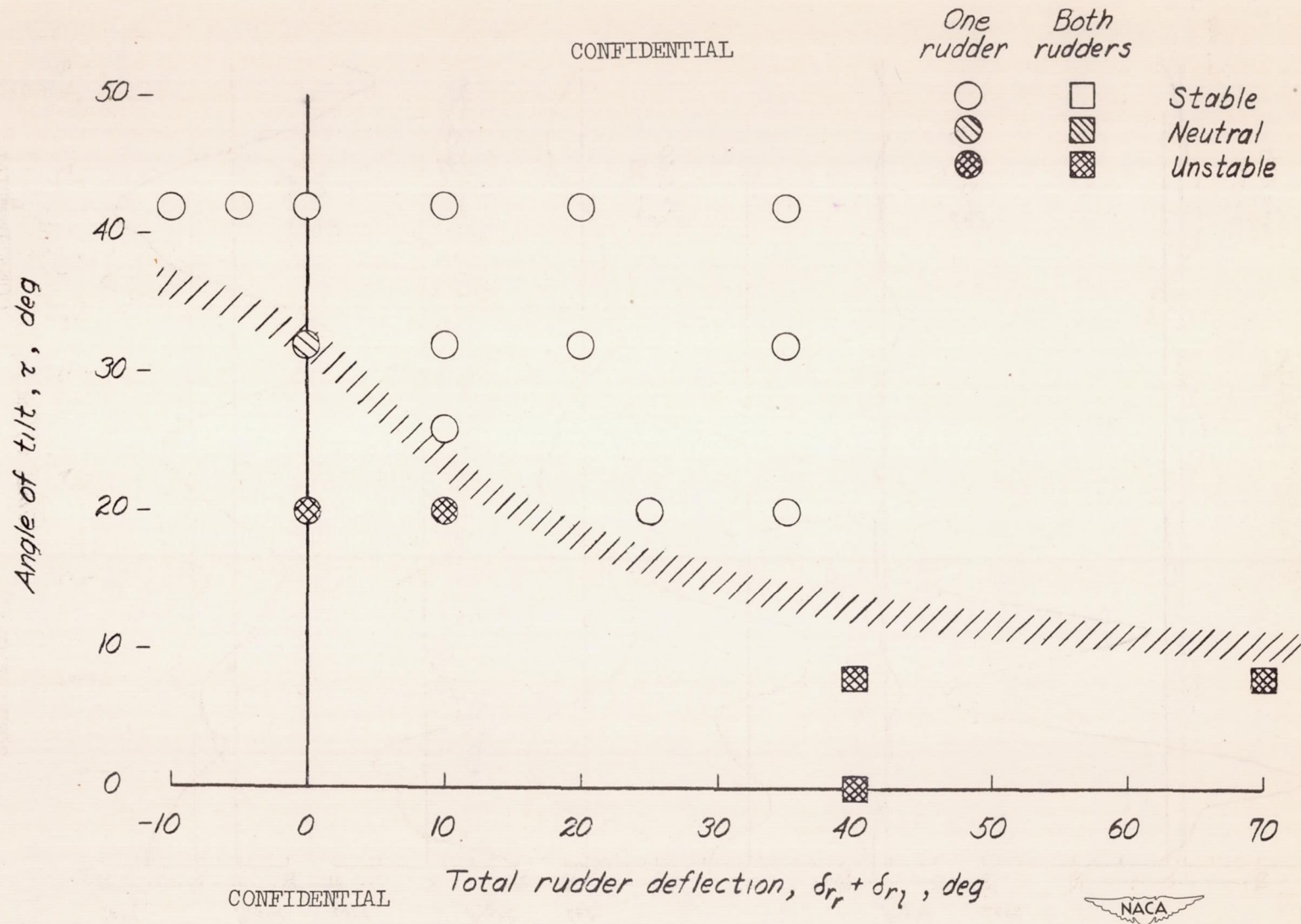


Figure 34.- Experimentally determined lateral stability boundary of the model.

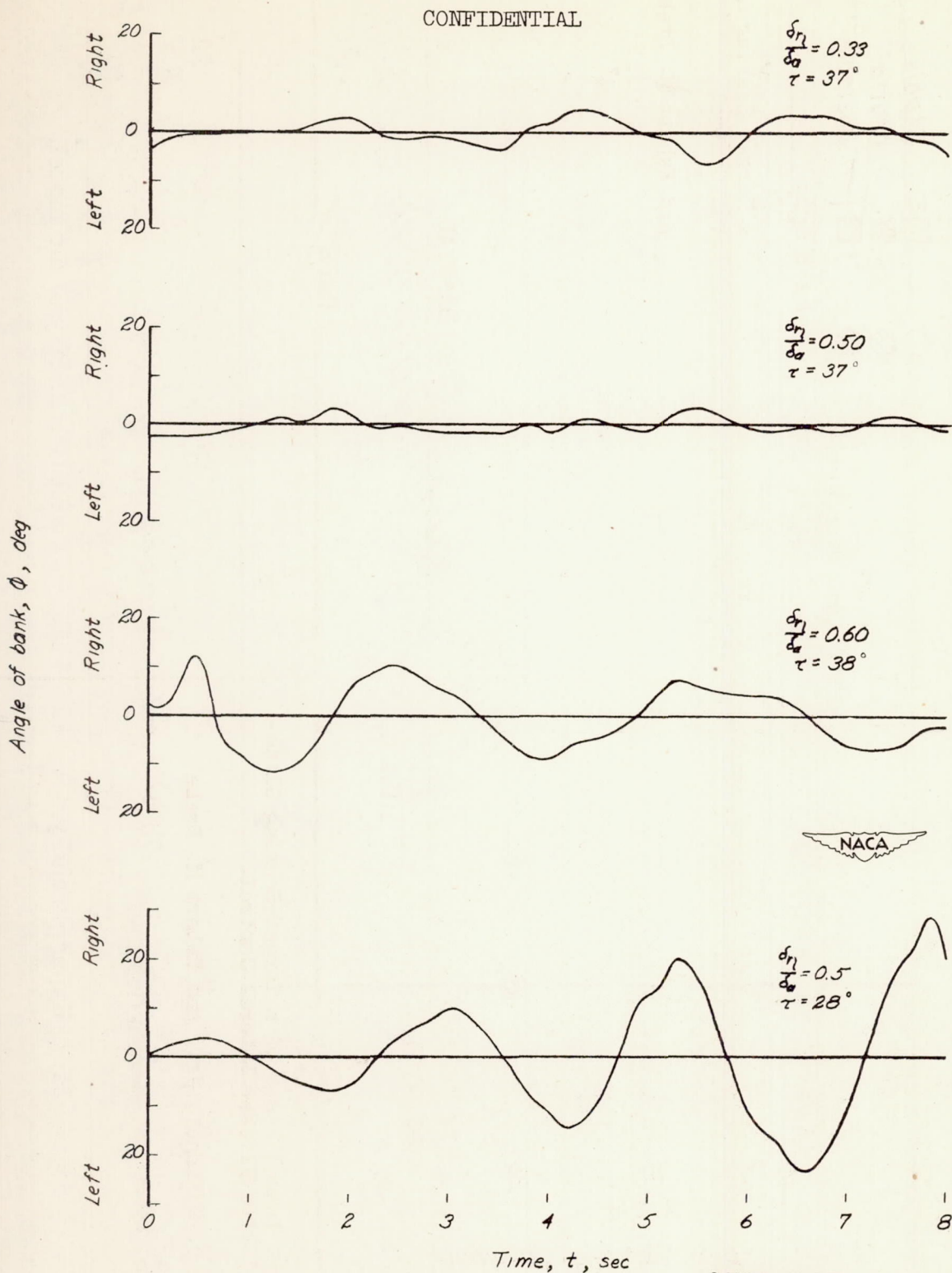


Figure 35.- Time histories of the rolling motions of the model with a proportional control system showing the effects of varying the angle of tilt and the ratio of rudder deflection to aileron deflection (taken from reference 1).